

# Magnetosphere-Ionosphere Coupling Through $E$ -region Turbulence: Energy Budget

Y. S. Dimant and M. M. Oppenheim

## Abstract.

During periods of intense geomagnetic activity, strong electric fields and currents penetrate from the magnetosphere into high-latitude ionosphere where they dissipate energy, form electrojets, and excite plasma instabilities in the  $E$ -region ionosphere. These instabilities give rise to plasma turbulence which induces non-linear currents and strong anomalous electron heating (AEH) as observed by radars. These two effects can increase the global ionospheric conductances. This paper analyzes the energy budget in the electrojet, while the companion paper applies this analysis to develop a model of anomalous conductivity and frictional heating useful in large-scale simulations and models of the geospace environment. Employing first principles, this paper proves for the general case an earlier conjecture that the source of energy for plasma turbulence and anomalous heating equals the work by external field on the non-linear current. Using a two-fluid model of an arbitrarily magnetized plasma and the quasilinear approximation, this paper describes the energy conversion process, calculates the partial sources of anomalous heating, and reconciles the apparent contradiction between the inherently 2-D non-linear current and the 3-D nature of AEH.

## 1. Introduction

At high latitudes, the large-scale electric field,  $\vec{E}_0$ , from the solar wind and Earth's magnetosphere penetrates to the ionosphere. Across the  $E$ /upper- $D$ -region altitudes, roughly between 80 and 130 km, the electrons are strongly magnetized, while the ions become at least partially demagnetized due to frequent collisions with the neutral atmosphere. This demagnetization slows the drifting ions down, making the  $\vec{E}_0 \times \vec{B}_0$  drift of electrons into strong Hall currents named high-latitude electrojets. In the global picture of magnetosphere-ionosphere (MI) coupling, this is the region where field-aligned magnetospheric currents close and dissipate energy.

Electrojet currents often drive plasma instabilities that generate electrostatic field fluctuations coupled to plasma density irregularities. These fluctuations have low frequencies, usually smaller than the average frequencies of electron and ion collisions with neutrals,  $\nu_{e,i}$ , while the corresponding wavelengths in the unstable range exceed the ion mean free path. Density irregularities, usually in the range from tens of centimeters to tens of meters, are routinely detected as strong coherent radar echoes [e.g., *Cohen and Bowles*, 1967; *Balsley and Farley*, 1971; *Crochet et al.*, 1979; *Kudeki et al.*, 1987]. Rocket flights through the lower ionosphere have detected also electrostatic field fluctuations [e.g., *Pfaff et al.*, 1987, 1992, 1997; *Rose et al.*, 1992; *Fukao et al.*, 1998]. These irregularities and fluctuations are caused by variety of instabilities including the Farley-Buneman (FB) [*Farley*, 1963; *Buneman*, 1963], gradient drift [*Hoh*, 1963; *Maeda et al.*, 1963], and thermal instabilities [*Dimant and Sudan*, 1995, 1997; *Kagan and Kelley*, 2000; *Dimant and Oppenheim*, 2004]. The FB instability is excited when the relative velocity between the average electron and ion streams exceeds the local ion-acoustic speed. At high latitudes, this usually occurs when  $E_0 \equiv |\vec{E}_0|$  exceeds the threshold value of about 20 mV/m. These and much stronger fields are not

uncommon in the sub-auroral, auroral, and polar cap areas, especially during magnetospheric storms and substorms.

Small-scale fluctuations generated by these instabilities can cause enormous anomalous electron heating (AEH). For about thirty years, radars have observed strong electron temperature elevations from 300-500 K up to more than 4000 K, correlating with strong convection fields  $\vec{E}_0$  [*Schlegel and St.-Maurice*, 1981; *Providakes et al.*, 1988; *Stauning and Olesen*, 1989; *St.-Maurice et al.*, 1990; *Williams et al.*, 1992; *Foster and Erickson*, 2000; *Bahcivan*, 2007]. Simple estimates show that regular ohmic heating by  $\vec{E}_0$  alone cannot account in full measure for such huge temperature elevations. A strong correlation between AEH and  $E_0$ , as well as other physical arguments, shows that average heating by FB-generated turbulent electric fields causes AEH [*St.-Maurice and Laher*, 1985; *Robinson*, 1986, 1992; *Providakes et al.*, 1988; *St.-Maurice*, 1987, 1990; *Dimant and Milikh*, 2003]. AEH occurs largely because the turbulent electrostatic field,  $\delta\vec{E} = -\nabla\delta\Phi$ , has a small component  $\delta\vec{E}_{||}$  parallel to the geomagnetic field  $\vec{B}_0$  [*St.-Maurice and Laher*, 1985; *Providakes et al.*, 1988; *Dimant and Milikh*, 2003; *Milikh and Dimant*, 2003; *Bahcivan et al.*, 2006]. The importance of  $\delta\vec{E}_{||}$  makes the entire process fully 3-D.

Anomalous electron heating can modify ionospheric conductances and hence affect the coupling between the magnetosphere and ionosphere. Any electron heating directly affects the temperature-dependent electron-neutral collision frequency and, hence, the electron part of the Pedersen conductivity. This part, however, is usually small compared to the electron Hall and ion Pedersen conductivities. However, AEH causes a gradual elevation of the mean plasma density within the anomalously heated regions by reducing the local plasma recombination rate [*Gurevich*, 1978; *St.-Maurice*, 1990; *Dimant and Milikh*, 2003; *Milikh et al.*, 2006]. The AEH-induced plasma density elevations increase all conductivities in proportion. However, this mechanism requires tens of seconds or even minutes because of the slow development of the ionization-recombination equilibrium. If  $\vec{E}_0$  changes faster than the characteristic recombination timescale then its time-averaged effect on density will be smoothed and reduced.

Plasma turbulence, however, can directly modify local ionospheric conductivities via a wave-induced non-linear

current (NC) associated with plasma density irregularities [Rogister and Jamin, 1975; Oppenheim, 1997; Buchert *et al.*, 2006]. The physical nature of the NC is explained in Fig. 1 for magnetized electrons and unmagnetized ions. The wave field,  $\delta\vec{E}$ , has different signs in the wave density maxima and minima, so that the corresponding  $\delta\vec{E} \times \vec{B}_0$ -drifts of magnetized electrons have opposite directions. As a result, more electrons drift along the maxima than in the opposite direction along the minima, producing a net non-linear current density,  $\vec{j}_{\text{NC}}$ . At higher  $E$ -region altitudes, partially magnetized ions can also contribute to this current. Relative density perturbations in saturated FB turbulence may reach at most tens percent, while the rms turbulent field,  $\langle\delta\vec{E}^2\rangle^{1/2}$ , is comparable to  $E_0$  (the angular brackets here and below denote spatial-temporal averaging). As a result, the total NC, considered as a plasma response to the external electric field  $\vec{E}_0$ , amounts to only a fraction of the regular electrojet Hall current. However, in most of the electrojet the NC is directed largely parallel to  $\vec{E}_0$ , so that it may increase significantly the much smaller Pedersen conductivity. This is critically important because the Pedersen conductivity allows the MI field-aligned currents to close and dissipate energy. The combined effect of the NC and AEH makes the ionosphere less resistive. The anomalous conductance may, at least partially, account for systematic overestimates of the total cross-polar cap potential in global MHD models that employ laminar conductivities [e.g., Winglee *et al.*, 1997; Raeder *et al.*, 1998, 2001; Siscoe *et al.*, 2002; Ober *et al.*, 2003; Merkin *et al.*, 2005a, b, 2007; Guild *et al.*, 2008; Wang *et al.*, 2008].

Furthermore, the NC and AEH are intrinsically related. As discussed in this paper, the work by the external DC electric field on the total current equals the total field energy input to ionosphere (total Joule heating), including that responsible for AEH. On the other hand, the total frictional

heating of electrons and ions effectively increases wave dissipation and reduces the turbulence intensity, thus affecting the NC.

The process of anomalous energy deposition from the magnetosphere to ionosphere has been recently studied by Buchert *et al.* [2006]. They showed that the apparent average turbulent energy deposition per unit volume and time,  $\langle\delta\vec{E} \cdot \delta\vec{j}\rangle$ , equals zero (here  $\delta\vec{j}$  is the fluctuation of the total current density  $\vec{j}$ ; a number of notations in this paper differ from those of Buchert *et al.* [2006]). The authors deduced that the total energy per unit volume and time lost by the external field  $\vec{E}_0$  to particles equals the total work performed by this field on the total average current,  $\vec{j} = \vec{j}_0 + \vec{j}_{\text{NC}}$  ( $\vec{j}_0$  is the laminar current density). They suggested that the actual energy input for the instability development and turbulence-induced energy losses equals  $\vec{E}_0 \cdot \vec{j}_{\text{NC}}$ . Their calculations supported this remarkable conjecture, but provided no complete proof since their quantitative analysis was based on an oversimplified and restrictive model. First and most importantly, they studied only 2-D turbulence in a perpendicular to  $\vec{B}_0$  plane. The authors did not state the 2-D restriction explicitly, but it becomes evident from their Eqs. (17) and (18) which effectively exclude  $\vec{k}_{\parallel}$ . Due to this, their treatment leaves out the key 3-D energy conversion process primarily responsible for AEH. Secondly, they employed the simplest two-fluid model with fully demagnetized ions. This widely used approximation is good for most of the electrojet but fails at its top part, right where the Pedersen conductivity reaches its maximum. Thirdly, their calculations of NC and other average terms were fully based on a quasilinear, narrowband approximation for FB waves. In this approximation, turbulence consists of relatively small-amplitude waves which are described by linear relations with narrowband wave frequencies. In many cases, this is a reasonable approach, although its applicability is less justified for the driving electric field well above the instability threshold, when the effect of AEH is especially strong.

These restrictions and some inconclusiveness associated with them raise a number of important questions. First and foremost, is the conjecture about  $\vec{E}_0 \cdot \vec{j}_{\text{NC}}$  as the energy input for plasma turbulence really true? If so, then this fundamental fact should follow directly from the first principles and be universally applicable. In particular, it has to be valid for arbitrarily magnetized particles and strongly non-linear processes. Then, is it possible to deduce this fact from a general viewpoint with no or minimal approximations? Second, presuming that  $\vec{E}_0 \cdot \vec{j}_{\text{NC}}$  is the correct energy input, then how is it compatible with the 3-D effect of AEH largely associated with small  $\delta E_{\parallel}$ ? This question arises because  $\vec{j}_{\text{NC}}$ , as well as  $\vec{E}_0$ , lies almost precisely in the plane perpendicular to  $\vec{B}_0$  with no average contribution from  $\vec{k}_{\parallel}$ . Recently, we performed a number of 2-D and 3-D particle-in-cell (PIC) simulations in big periodic boxes with unprecedentedly dense meshes and large numbers of PIC particles [Oppenheim *et al.*, 2011]. Comparing the 2-D and 3-D results for the same background parameters, we have obtained compelling evidence that anomalous electron heating related to plasma structuring along  $\vec{B}_0$  does exist. Then, how could essentially 3-D heating originate from the 2-D energy input? Further, how this energy input is distributed between various groups of particles? This is important for making accurate estimates of anomalous heating for different particle groups. During strong magnetospheric events, what feedback of developed  $E$ -region turbulence on global MHD behavior of the magnetosphere might be expected? How to quantify this effect for including it in global MHD codes intended for space weather predictions? Finally, what channels provide the corresponding energy flow between the magnetosphere and  $E/D$ -region ionosphere?

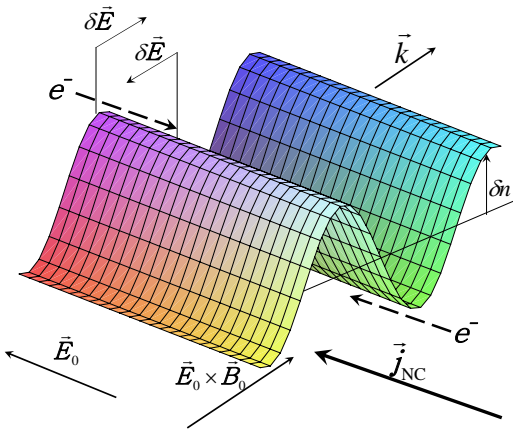


**Figure 1.** Formation of a net non-linear current (NC) at a given wave of plasma compression/decompression with the wavevector  $\vec{k}$  in the  $\vec{E}_0 \times \vec{B}_0$ -direction. The wave electrostatic field,  $\delta\vec{E} \parallel \vec{k}$ , has opposite directions in the plasma density maxima ( $\delta n > 0$ ) and minima ( $\delta n < 0$ ), resulting in the oppositely directed  $\delta\vec{E} \times \vec{B}_0$  drifts of magnetized electrons. More negatively charged particles move in the  $-\vec{E}_0$  than those in the opposite direction, resulting in formation of the net positive current,  $\vec{j}_{\text{NC}}$ , parallel to  $\vec{E}_0$ .

In this paper, we address these issues and create a rigorous basis for calculating anomalous conductivities in the companion paper [Dimant and Oppenheim, 2011]. We start by confirming from first principles that fully saturated turbulence does yield  $\langle \delta \vec{E} \cdot \delta \vec{j} \rangle = 0$ , then confirm the *Buchert et al.* [2006] deduction regarding the turbulent energy input and establish its universal validity. In order to quantitatively develop a 3-D model of AEH and resolve the apparent contradiction between this interpretation and the 2-D nature of the energy input, we perform specific calculations for the case of arbitrary particle magnetization, using a quasilinear approximation. We calculate the non-linear current, total energy input, and partial average frictional heating sources for both electrons and ions in terms of a given spectrum of density irregularities. We show that the major quantitative difference between 2-D and 3-D developed turbulence lies in the magnitude of density perturbations. These perturbations and the non-linear current proportional to them are noticeably larger in 3-D than in 2-D. This difference explains the larger energy input in 3-D and is responsible for AEH caused by turbulent fields, thus resolving the above-mentioned contradiction.

The paper is organized as follows. In Sect. 2, using only first principles with no approximations, we confirm for the general case the *Buchert et al.* [2006] findings regarding the energy input. In Sect. 3, we develop a quasilinear approach, similar to that of *Buchert et al.* [2006], but for the general 3-D case of arbitrarily magnetized particles. This allows us to calculate partial non-linear currents, relevant energy inputs, and frictional heating sources. In Sect. 4, we discuss global energy flow between the magnetosphere and ionosphere. In the appendix, we check the validity of the conventional electrostatic approximation for lower-ionosphere wave processes.

## 2. Energy Conversion: First Principle Consideration

In this section, we derive general relations regarding the average energy input in quasi-periodic systems and show how the *Buchert et al.* [2006] deductions follow from fundamental electrodynamic and plasma kinetics principles with no approximations like electrostatics, quasi-neutrality, fluid-model description, etc.

First, we consider the evolution of the field energy in plasmas by considering the exact electrodynamics, starting with Ampere's and Faraday's laws,

$$\partial_t \vec{E} = c^2 (\nabla \times \vec{B}) - \frac{\vec{j}}{\varepsilon_0}, \quad (1a)$$

$$\partial_t \vec{B} = -\nabla \times \vec{E}, \quad (1b)$$

where  $\varepsilon_0$  is the permittivity of free space,  $c$  is the speed of light in vacuum,  $\vec{E}$  and  $\vec{B}$  are the electric field and magnetic induction, and  $\vec{j}$  is the total current density.

Taking scalar products of Eq. (1a) with  $\varepsilon_0 \vec{E}$ , Eq. (1b) with  $\varepsilon_0 c^2 \vec{B}$  and adding the results, we obtain the standard energy balance equation (aka Poynting's theorem):

$$\partial_t U + \nabla \cdot \vec{S} = -\vec{E} \cdot \vec{j}, \quad (2)$$

where

$$U = \frac{\varepsilon_0}{2} (E^2 + c^2 B^2), \quad \vec{S} \equiv \frac{\vec{E} \times \vec{B}}{\mu_0} \quad (3)$$

are the field energy density and the corresponding flux (the Poynting vector), respectively;  $\mu_0 = (\varepsilon_0 c^2)^{-1}$  is the permeability of free space.

Now we need to find  $\vec{j}$  from the plasma. The dynamics of individual particles of type  $s$ , such as electrons or ions ( $s = e, i$ ), is accurately described by Boltzmann's kinetic

equation, which can be written in the 6-D divergence form as

$$\partial_t f_s + \nabla \cdot (\vec{v}_s f_s) + \partial_{\vec{v}_s} \cdot \left[ \frac{q_s}{m_s} (\vec{E} + \vec{v}_s \times \vec{B}) f_s \right] = S_s. \quad (4)$$

Here  $\vec{v}_s$  is the kinetic velocity of the particles- $s$ , while  $f_s(\vec{r}, t, \vec{v}_s)$  is their single-particle velocity distribution function normalized to the particle- $s$  density,  $n_s \equiv \int f_s d^3 v_s$  (the integration here and below is performed over the entire 3-D velocity space);  $q_s$  and  $m_s$  are the particle charge and mass;  $S_s$  is the collisional operator which includes particle-particle collisions and can also include the ionization sources and recombination losses; for simplicity, we disregard effects of gravity. Multiplying Eq. (4) by  $m_s v_s^2/2$ , integrating over the velocity space, and adding the results for all plasma particles, we obtain the energy balance relation for plasma,

$$\partial_t \sum_s \mathcal{E}_s + \nabla \cdot \sum_s \vec{K}_s = \vec{E} \cdot \vec{j} + \sum_s L_s. \quad (5)$$

Here  $\mathcal{E}_s \equiv \int (m_s v_s^2/2) f_s d^3 v_s$  and  $\vec{K}_s \equiv \int (m_s v_s^2/2) \vec{v}_s f_s d^3 v_s$  are the average particle energy and energy-flux densities, respectively;  $L_s \equiv \int (m_s v_s^2/2) S_s d^3 v_s$  combines all collisional energy gains and losses;  $\vec{j} \equiv \sum_s q_s n_s \vec{V}_s$ , is the total current density, the same as in Eq. (2);  $\vec{V}_s \equiv \int \vec{v}_s f_s d^3 v_s / n_s$  is the particle- $s$  mean fluid velocity. In the general case, the particle-energy density  $\mathcal{E}_s$  combines the mean thermal energy,  $3n_s T_s/2$ , where  $T_s \equiv \int [m_s (v_s - \vec{V}_s)^2/3] f_s d^3 v_s / n_s$  is the effective particle temperature, with the kinetic energy density of the mean particle flow,  $n_s m_s V_s^2/2$ .

Comparison of Eqs. (2) and (5) shows that  $\vec{E} \cdot \vec{j}$  is the total energy input from the fields to particles per unit volume and time. The energy deposited in an individual group of particles at a given location may be then slightly redistributed via Coulomb collisions and transported to other locations. Eventually, this energy becomes lost to the abundant neutral atmosphere via predominantly inelastic plasma-neutral collisions.

General Eqs. (2) and (5) apply to all plasma processes, linear or non-linear. To specifically discuss turbulent processes, we need to separate them from the slowly evolving and large-scale regular background structures and processes. This can be done by using a conventional two-scale approach in which macroscopic background structures and processes are presumed to have much longer characteristic spatial and temporal scales than does the turbulence. The physical conditions in the  $E$ -region plasma make this procedure more applicable to plasma irregularities generated by local instability mechanisms, such as the Farley-Buneman (FB) and thermal-driven instabilities [Dimant and Sudan, 1997; Kagan and Kelley, 2000; Dimant and Oppenheim, 2004] than for relatively large-scale irregularities generated by plasma gradients.

We assume that plasma turbulence generated by instabilities consists mostly of waves whose wavelengths  $\lambda_i$  in each direction  $i$  are much smaller than the corresponding typical scales of spatial variation of the macroscopic background parameters,  $\Lambda_i$ . Then, for any given location  $\vec{r}$ , we can build an imaginary rectilinear box centered around  $\vec{r}$  with the sizes  $L_i$  that satisfy the conditions  $\lambda_i \ll L_i \ll \Lambda_i$ . The characteristic scales in different directions  $i$  can differ dramatically. For example, the wavelengths of nearly field-aligned irregularities parallel to  $\vec{B}_0$  are generally orders of magnitude larger than those perpendicular to  $\vec{B}_0$ , so that the corresponding box sizes would also be vastly different. Within the imaginary box, we can extend the background parameters from the box center  $\vec{r}$  uniformly to the entire box

and impose periodic boundary conditions. This approach is widely employed in computer simulations.

We can similarly describe the temporal evolution of the process by presuming long-lasting non-linearly saturated turbulence in a quasi-stationary background. This implies a continuous driving of instability and allows one to introduce a quasi-period  $T$ , analogous to  $L_i$ , which is much longer than typical timescales of turbulent variations but is much shorter than a characteristic timescale of slow evolution of the macroscopic background.

To implement the two-scale procedure, we introduce the following convention. We denote the short-scale and fast periodic variables for turbulent processes by  $\vec{x} = (x_1, x_2, x_3)$  and  $t$ , while denoting the corresponding coordinates and time of large-scale and slow background variations by  $\vec{r}$  and  $\tau$ , respectively. With respect to the periodic coordinates  $\vec{x}$  and time  $t$ , we define a spatial-temporal average as

$$\langle \cdots \rangle \equiv \frac{1}{L_1 L_2 L_3 T} \int_{-L_1/2}^{L_1/2} dx_1 \int_{-L_2/2}^{L_2/2} dx_2 \int_{-L_3/2}^{L_3/2} dx_3 \int_{\tau-T/2}^{\tau+T/2} dt. \quad (6)$$

In general, such averages can remain functions of the slow variables  $\vec{r}$  and  $\tau$ . This description of turbulence does not require the ensemble averaging employed by *Buchert et al.* [2006].

Having implemented this procedure, we split the quasi-periodic fields and currents into their  $\vec{r}, \tau$ -dependent average parts and the corresponding local periodic perturbations,

$$\vec{E} = \langle \vec{E} \rangle + \delta \vec{E}, \quad \vec{B} = \langle \vec{B} \rangle + \delta \vec{B}, \quad \vec{j} = \langle \vec{j} \rangle + \delta \vec{j}, \quad (7)$$

Using  $\langle \delta \vec{E} \rangle = \langle \delta \vec{j} \rangle = 0$ , we obtain for the average energy deposition term

$$\langle \vec{E} \cdot \vec{j} \rangle = \langle \vec{E} \rangle \cdot \langle \vec{j} \rangle + \langle \delta \vec{E} \cdot \delta \vec{j} \rangle. \quad (8)$$

One might naively interpret the first term on the right-hand side (RHS) of Eq. (8) as the energy input from the background fields to the undisturbed plasma, while the second term as the corresponding average contribution from the turbulent fields. As mentioned in the Introduction, *Buchert et al.* [2006] found, using a simplified model, that  $\langle \delta \vec{E} \cdot \delta \vec{j} \rangle$  equals zero by the following formal mathematical reason. If one expands this term further in terms of the mean particle fluid velocities to the lowest-order quadratic non-linearity then the expected total turbulent frictional heating term,  $\sum_s q_s n_{s0} \langle \delta \vec{E} \cdot \delta \vec{V}_s \rangle$ , turns out to be automatically canceled by a density perturbation term,  $\sum_s q_s \langle \delta n_s \delta \vec{E} \rangle \cdot \vec{V}_{s0}$  (here  $\delta n_s$  and  $\delta \vec{V}_s$  are the perturbations of the densities and particle fluid velocities). Right below we show that for purely periodic and spatially homogeneous turbulence the equality  $\langle \delta \vec{E} \cdot \delta \vec{j} \rangle = 0$  is a natural and universal constraint, required merely by the imposed periodicity. This constraint follows directly from exact Maxwell's equations without invoking specific plasma models.

Indeed, Maxwell's equations are linear, allowing the separation of the average quantities from wave perturbations. The perturbations depend on the small-scale, quasi-periodic variables,  $\vec{x}$ ,  $t$ , and can also have an adiabatically slow  $\vec{r}$ ,  $\tau$ -dependence due to background inhomogeneities and evolution. In principle, the inhomogeneous background parameters may evolve in such a way that an instability threshold is crossed, resulting in sudden onset or disappearance of instability in some locations at certain moments of time. Such instances, analogous to second-order phase transitions [*Landau and Lifshitz*, 2000], break the validity of our two-scale approximation and deserve a special treatment that lies beyond the framework of this paper. Apart from these special occasions, we can apply to the perturbations of the fields and current the same steps that lead to Eq. (2). Averaging

the result in accord with the definition of Eq. (6), we obtain

$$\partial_\tau \left[ \frac{\varepsilon_0 (\langle \delta E^2 \rangle + c^2 \langle \delta B^2 \rangle)}{2} \right] + \nabla_{\vec{r}} \cdot \frac{\langle \delta \vec{E} \times \delta \vec{B} \rangle}{\mu_0} = -\langle \delta \vec{E} \cdot \delta \vec{j} \rangle. \quad (9)$$

Then for saturated turbulence with constant average characteristics in a strictly periodic box, the left-hand side (LHS) of Eq. (9) disappears, yielding

$$\langle \delta \vec{E} \cdot \delta \vec{j} \rangle = 0, \quad (10)$$

regardless of the specific fluid or kinetic models employed for the plasma description. For strictly periodic processes, this result is exact. One can also obtain it directly from the discrete Fourier harmonics of the electric field and current. We do this right below and also demonstrate that electrostatic and quasi-neutral approximations do not lift this exact electrodynamic constraint.

We start by introducing spatial and temporal Fourier harmonics of wave perturbations for general, linear or non-linear, periodic processes. Since we imply saturated turbulence in a 4-D box (3-D space + time) with periodic boundary conditions, it is logical to employ the 4-D discrete Fourier transformation. For easy reading, we assign to the Fourier transforms the notations of the original variables but with additional subscripts  $\vec{k}, \omega$ . For a scalar or vector periodic perturbation  $\delta F(\vec{x}, t)$  as a function of coordinates  $x_i$  and time  $t$ , we define such transformations within the 4-D box of the corresponding sizes  $L_i$  and the quasi-period  $T$  as

$$\delta F(\vec{x}, t) = \sum_{\vec{k}, \omega \neq 0} \delta F_{\vec{k}, \omega} \exp[i(\vec{k} \cdot \vec{x} - \omega t)], \quad (11a)$$

$$\delta F_{\vec{k}, \omega} = \frac{1}{L_1 L_2 L_3 T} \int \delta F(\vec{x}, t) \exp \left[ -i \left( \sum_{i=1}^3 k_i x_i - \omega t \right) \right] d^3 x_i dt. \quad (11b)$$

Here the  $\vec{k}, \omega \neq 0$  summation is taken over all discrete values of  $\vec{k}$ ,  $k_i = 2\pi n_i / L_i$ ,  $\omega = 2\pi m / T$ , with integer  $n_i$ ,  $m$ , while the integration is performed over the entire 4-D box, as in Eq. (6). Since we apply the discrete Fourier transforms only to the perturbations, we exclude from the summation over harmonics the average values corresponding to  $\vec{k}, \omega = 0$ . In terms of their Fourier harmonics,  $\delta A_{\vec{k}, \omega}$  and  $\delta B_{\vec{k}, \omega}$ , the spatial-temporal average of any product, scalar or vector, of two functions  $A(\vec{x}, t)$  and  $B(\vec{x}, t)$ , is given by

$$\langle \delta A(\vec{x}, t) \delta B(\vec{x}, t) \rangle = \sum_{\vec{k}, \omega \neq 0} \delta A_{\vec{k}, \omega} \delta B_{\vec{k}, \omega}^* = \sum_{\vec{k}, \omega \neq 0} \delta A_{\vec{k}, \omega}^* \delta B_{\vec{k}, \omega}. \quad (12)$$

Our current discrete-transform normalization differs from the continuous one in *Buchert et al.* [2006] and allows to avoid the emergence of extraneous factors like  $VT$  ( $V = L_1 L_2 L_3$ ) and  $(2\pi)^4$  in the explicit physical expressions for average quadratically non-linear quantities [e.g., *Buchert et al.*, 2006, Eqs. (6)–(8), (19)–(26), etc.].

Using Fourier transforms, we now prove Eq. (10) in a more direct way. Applying Eq. (11) to Eq. (1), for a given Fourier harmonic, we obtain

$$ic^2 \vec{k} \times \delta \vec{B}_{\vec{k}, \omega} = \frac{1}{\varepsilon_0} \delta \vec{j}_{\vec{k}, \omega} - i\omega \delta \vec{E}_{\vec{k}, \omega}, \quad i\vec{k} \times \delta \vec{E}_{\vec{k}, \omega} = i\omega \delta \vec{B}_{\vec{k}, \omega}. \quad (13)$$

Making a cross-product of Eq. (13) with  $\vec{k}$  and using  $\vec{k} \cdot \delta \vec{B}_{\vec{k}, \omega} = 0$ , we express the field perturbations in terms of

$$\delta \vec{j}_{\vec{k},\omega},$$

$$\delta \vec{E}_{\vec{k},\omega} = \frac{i\vec{k} \times \delta \vec{j}_{\vec{k},\omega}}{\varepsilon_0(k^2 c^2 - \omega^2)}, \quad (14)$$

$$\delta \vec{E}_{\vec{k},\omega} = \frac{i \left[ \omega^2 \delta \vec{j}_{\vec{k},\omega} - c^2 (\vec{k} \cdot \delta \vec{j}_{\vec{k},\omega}) \vec{k} \right]}{\varepsilon_0 \omega (k^2 c^2 - \omega^2)}. \quad (15)$$

In a long-lived quasi-periodic non-linearly saturated state, all wave frequencies  $\omega$  must be real, so that Eq. (15) yields  $\text{Re}(\delta \vec{E}_{\vec{k},\omega} \cdot \delta \vec{j}_{\vec{k},\omega}^*) = 0$ , i.e., Eq. (10).

General Eq. (10) represents a strict constraint that follows from the full electrodynamics of quasi-periodic processes, but it is not obvious that it should hold for the electrostatic and quasi-neutrality approximations. The following demonstrates that these approximations do not lift this constraint.

Indeed, the electron and ion continuity equations combined yield  $e\partial_t(\delta n_e - \delta n_i) = \nabla \cdot \delta \vec{j}$ , so that  $e\omega(\delta n_{e,\omega} - \delta n_{i,\omega}) = \vec{k} \cdot \delta \vec{j}_{\vec{k},\omega}$ . Combining this with Poisson's equation,  $\varepsilon_0 \nabla \cdot \delta \vec{E} = e(\delta n_e - \delta n_i)$ , we obtain

$$i\vec{k} \cdot \delta \vec{E}_{\vec{k},\omega} = \frac{\vec{k} \cdot \delta \vec{j}_{\vec{k},\omega}}{\varepsilon_0 \omega}. \quad (16)$$

For an electrostatic field, we have  $\delta \vec{E}_{\vec{k},\omega} = |\delta \vec{E}_{i\vec{k},\omega}|(\vec{k}/k)$ , so that Eqs. (12) and (16) yield

$$\langle \delta \vec{j} \cdot \delta \vec{E} \rangle = \text{Re}(\delta \vec{j}_{\vec{k},\omega} \cdot \delta \vec{E}_{\vec{k},\omega}^*) = -\varepsilon_0 |\delta \vec{E}_{\vec{k},\omega}|^2 \text{Im} \omega = 0. \quad (17)$$

If we add quasi-neutrality,  $\nabla \cdot \delta \vec{j} = 0$ , i.e.,  $\vec{k} \cdot \delta \vec{j}_{\vec{k},\omega} = 0$  for individual harmonics, then the satisfaction of Eq. (10) becomes obvious even without assumption of real  $\omega$ ,

$$\langle \delta \vec{j} \cdot \delta \vec{E} \rangle = i \sum_{\vec{k}, \omega \neq 0} (\vec{k} \cdot \delta \vec{j}_{\vec{k},\omega}) \delta \Phi_{\vec{k},\omega}^* = 0, \quad (18)$$

Equation (10) does not mean, however, that developed plasma turbulence makes no contribution to the average particle heating. This would certainly contradict both observations and PIC simulations. The paradox can be resolved as follows. The average electric field is merely the external field,  $\langle \vec{E} \rangle = \vec{E}_0$ , while  $\langle \vec{j} \rangle \neq \vec{j}_0$ , where  $\vec{j}_0 \equiv \sum_s q_s n_{s0} \vec{V}_{s0}$  is the undisturbed current density determined by the laminar plasma response to  $\vec{E}_0$ . In addition to  $\vec{j}_0$ , the total average current density,  $\langle \vec{j} \rangle$ , includes a wave-induced direct NC [Rogister and Jamin, 1975; Oppenheim, 1997; Buchert et al., 2006],

$$\vec{j}^{\text{NC}} = \langle \vec{j} \rangle - \vec{j}_0 \equiv \sum_s q_s \langle \delta n_s \delta \vec{V}_s \rangle. \quad (19)$$

The total average loss of field energy to particles per unit volume and time is given by  $\langle \vec{E} \cdot \vec{j} \rangle$ . The corresponding energy dissipation in the laminar ionosphere with no instabilities is given by  $\vec{E}_0 \cdot \vec{j}_0$ . Then the total energy dissipation exclusively due to plasma turbulence is  $L_{\text{turb}} \equiv \langle \vec{E} \cdot \vec{j} \rangle - \vec{E}_0 \cdot \vec{j}_0$ . Using Eqs. (10) and (19), one can easily establish that

$$L_{\text{turb}} = P_{\text{NC}} \equiv \vec{E}_0 \cdot \vec{j}^{\text{NC}}. \quad (20)$$

Thus, it is formally the work by the external electric field on the non-linear current,  $P_{\text{NC}}$ , rather than  $\langle \delta \vec{E} \cdot \delta \vec{j} \rangle$ , that provides the required turbulent energy deposition for all kinds of anomalous heating of plasma particles. Buchert et al. [2006] showed this for the restricted case of fluid plasmas with fully unmagnetized ions and a quasilinear wave description, but did not establish it in the general case. We have

just demonstrated that this fundamental result follows directly from the general field electrodynamics and no specific plasma models. By their physical meaning and according to Eq. (20) each of the two equal quantities  $L_{\text{turb}}$  and  $P_{\text{NC}}$  can be named “turbulent Joule heating.”

Rigorously speaking, exact Eqs. (10) and (20) apply only to a homogeneous and stationary background. For mildly inhomogeneous and slowly evolving background parameters, Eq. (9) can be treated using a regular perturbation technique. The zero-order approximation, corresponding to a given turbulence level within an isolated box with a uniform background and periodic boundary conditions and, hence, not affected by the outside inhomogeneity, yields Eq. (10). To reach a next-order accuracy, one has to establish the zero-order parameter dependence of non-linearly saturated turbulence characteristics, using, e.g., a series of computer simulations with periodic boundary conditions but various background parameters. Given the large-scale spatial dependence and slow evolution of the background parameters, one could calculate then the LHS of Eq. (9). This would yield the first-order, potentially non-zero, values for  $\langle \delta \vec{E} \cdot \delta \vec{j} \rangle$  on the RHS. Under applicability of our two-scale approach, however, such possible finite values of  $\langle \delta \vec{E} \cdot \delta \vec{j} \rangle$  will automatically be small compared to the nearly balancing each other leading terms in the expanded form of  $\langle \delta \vec{E} \cdot \delta \vec{j} \rangle$  with  $\delta \vec{j} = \sum_s q_s (\vec{V}_{s0} \delta n + n_0 \delta \vec{V}_s + \delta n \delta \vec{V}_s)$ , creating only a relatively small mismatch between  $L_{\text{turb}}$  and  $P_{\text{NC}}$ .

Below we calculate energies deposited among individual particle groups using an approach similar to that used by Buchert et al. [2006], except that we will apply it to a system with arbitrarily magnetized electrons and ions. This applies to all altitudes across the entire  $E$  region down to the upper  $D$  region. As mentioned above, Buchert et al. [2006] actually performed a 2-D treatment. We consider here fully 3-D turbulence, which is crucial for anomalous electron heating. Note that the total energy input spent on anomalous heating of plasma particles is less than  $P_{\text{NC}}$  because a fraction of the deposited energy via collisions goes directly to colliding neutrals and has no chance to heat the plasma.

### 3. Partial Energy Deposit: Quasilinear Approximation

In this section, we employ Fourier harmonics in a 3-D periodic box in order to identify the effect of the parallel turbulent electric field. Our results apply to all regions that contribute to the total ionospheric conductances, from the top electrojet down to the potentially unstable  $D$ -region [Kelley, 2009]. Similar processes can occur in other plasma media, like the Solar chromosphere [Liperovsky et al., 2000; Fontenla et al., 2008; Gogoberidze et al., 2009], other planetary ionospheres, and laboratory plasma [D’Angelo et al., 1974; John and Saxena, 1975; Koepke, 2008], despite the dramatic differences in parameters. Lastly, these calculations for arbitrarily magnetized plasma serve as an additional verification of the general relations obtained in the previous section from first principles.

In this paper, we restrict ionospheric particles to electrons and a single species of ions, adopting the quasi-neutrality,  $n_e \approx n_i = n$ . Similarly to Buchert et al. [2006], we apply here a quasilinear approximation, by which we imply that separate Fourier harmonics of predominantly electrostatic field and plasma density fluctuations are coupled through simple linear relations. Using these relations, we calculate then quadratically non-linear averages in terms of given spatial-temporal turbulence spectra.

This section is organized as follows. In Sect. 3.1, we obtain linear relationships to first-order accuracy and explain what we mean by the different orders. These first-order relations provide the linear wave frequencies and relations between the electrostatic potential and density perturbations.

In Sect. 3.2 we calculate the partial and total non-linear currents in terms of a given spectrum of irregularities. In Sect. 3.3, we calculate partial energy inputs and turbulent heating of electrons and ions and verify that general Eqs. (10) and (20) remain in this approximation exactly valid.

### 3.1. First-Order Linear Wave Relations

*Fejer et al.* [1984] studied the linear theory of collisional waves for strongly magnetized electrons and arbitrarily magnetized ions. On the other hand, *Buchert et al.* [2006] assumed arbitrarily magnetized electrons but unmagnetized ions. Since no one has published the general 3-D linear relations that cover all cases, we do this here and a more general version in the appendix of the companion paper [*Dimant and Oppenheim*, 2011]. In reasonable agreement with our PIC simulations, we assume that most of developed turbulence lies in the long-wavelength, low-frequency range of  $kl_i \ll 1$  and  $\omega \ll \nu_i$ , where  $\omega$  is the wave frequency and  $l_i$  is the mean free path of ions with respect to dominant ion-neutral collisions. This allows us to employ a two-fluid, as opposed to kinetic, model and order various terms in the momentum equations with respect to the small parameters  $kl_i$  and  $\omega/\nu_i$ . In this ordering, particle inertia and pressure gradients are second-order effects and can be neglected. This first-order approximation yields a dispersion relation and the corresponding relation between fluctuations of the plasma density and electrostatic potential. These relations are common for all  $E/D$ -region plasma instabilities [*Dimant and Oppenheim*, 2004]. The neglected second-order corrections are crucial for the linear wave dissipation and instability driving, but they are of less importance to the spatially/temporally averaged energy transfer and plasma heating. To the second-order accuracy, the general linear wave theory for arbitrarily magnetized plasmas is developed in the appendix of *Dimant and Oppenheim* [2011].

Though we discuss here the linear wave relationships, that does not mean that we consider the linear stage of instability. On the contrary, we assume a fully developed and non-linearly saturated turbulence in which the linear wave growth is balanced by non-linearities. However, we presume that these non-linearities only weakly modify the linear wave relationships, so that we include all non-linear terms, along with the instability driving or damping terms, into the second-order corrections and neglect their feedback on the first-order relations.

Under the first-order approximation, each group of particles has only two balancing forces: the Lorentz force and resistive collisional friction,

$$q_s(\vec{E} + \vec{V}_s \times \vec{B}) = m_s \nu_s \vec{V}_s, \quad (21)$$

where  $s = e, i$ ; we presume  $V_s$  lies a neutral frame of reference and an undisturbed magnetic field,  $\vec{B} = \vec{B}_0$ . Introducing the conventional magnetization parameters,  $\kappa_s \equiv \Omega_s/\nu_s$ , where  $\Omega_s = |q_s|B/m_s$  are the electron and ion gyrofrequencies, we obtain from Eq. (21)

$$\vec{V}_{e\parallel} = -\frac{\kappa_e \vec{E}_{\parallel}}{B}, \quad \vec{V}_{i\parallel} = \frac{\kappa_i \vec{E}_{\parallel}}{B}, \quad (22)$$

$$\vec{V}_{e\perp} = \frac{\kappa_e [-\vec{E}_{\perp} + \kappa_e (\vec{E} \times \hat{b})]}{(1 + \kappa_e^2) B}, \quad \vec{V}_{i\perp} = \frac{\kappa_i [\vec{E}_{\perp} + \kappa_i (\vec{E} \times \hat{b})]}{(1 + \kappa_i^2) B}, \quad (23)$$

with the subscripts  $\parallel, \perp$  denoting the components parallel and perpendicular to  $\vec{B}$ , respectively; here  $B \equiv |\vec{B}|$  and  $\hat{b} \equiv \vec{B}/B$ .

Further, we calculate the relative mean velocity between electrons and ions,  $\vec{U} \equiv \vec{V}_e - \vec{V}_i$ , which plays an important

role in many relations. Equations (22) and (23) give

$$\vec{U}_{\parallel} = -\frac{(\kappa_e + \kappa_i) \vec{E}_{\parallel}}{B}, \quad (24a)$$

$$\vec{U}_{\perp} = \frac{(\kappa_e + \kappa_i) [(\kappa_e - \kappa_i) (\vec{E} \times \hat{b}) - (1 + \kappa_i \kappa_e) \vec{E}_{\perp}]}{(1 + \kappa_e^2)(1 + \kappa_i^2) B}. \quad (24b)$$

Reversing Eq. (24), we obtain

$$\begin{aligned} \frac{\vec{E}_{\parallel}}{B} &= -\frac{\vec{U}_{\parallel}}{\kappa_e + \kappa_i}, \\ \frac{\vec{E}_{\perp}}{B} &= -\frac{(\kappa_e - \kappa_i) (\vec{U} \times \hat{b}) + (1 + \kappa_i \kappa_e) \vec{U}_{\perp}}{\kappa_i + \kappa_e}, \end{aligned} \quad (25)$$

so that Eqs. (22) and (23) yield the following mean drift velocities of electrons and ions in terms of their relative velocity:

$$\vec{V}_{e\parallel} = \frac{\kappa_e \vec{U}_{\parallel}}{\kappa_e + \kappa_i}, \quad \vec{V}_{i\parallel} = -\frac{\kappa_i \vec{U}_{\parallel}}{\kappa_e + \kappa_i}, \quad (26)$$

$$\vec{V}_{e\perp} = \frac{\kappa_e [\vec{U}_{\perp} - \kappa_i (\vec{U} \times \hat{b})]}{\kappa_e + \kappa_i}, \quad (27a)$$

$$\vec{V}_{i\perp} = -\frac{\kappa_i [\vec{U}_{\perp} + \kappa_e (\vec{U} \times \hat{b})]}{\kappa_e + \kappa_i}. \quad (27b)$$

All these linear expressions can be applied separately to the undisturbed quantities and wave perturbations.

Now we consider wave perturbations of the field, plasma density, and fluid velocities and apply to them the discrete Fourier transforms introduced by Eq. (11). Note that the neglect of non-linear terms with respect to wave perturbations leads to a unique  $\vec{k}$ -dependence of the wave frequency,  $\omega = \omega_{\vec{k}}(\vec{k})$ , via the corresponding first-order linear dispersion relation. Such unique dependence may break the presumed discreteness of the wave frequency,  $\omega = 2\pi m/T$ . However, the quasi-period  $T$  can always be chosen sufficiently long so that the interval between adjacent discrete frequencies,  $\Delta\omega = 2\pi/T$ , becomes much less than the finite spectral width around  $\omega = \omega_{\vec{k}}$ ; see also the discussion below in the paragraph following Eq. (40).

Expressing velocity perturbations,  $\delta\vec{V}_{e,i\vec{k},\omega}$ , in terms of the electrostatic potential perturbations,  $\delta\Phi_{\vec{k},\omega}$ , via  $\delta\vec{E}_{\vec{k},\omega} = -i\vec{k}\delta\Phi_{\vec{k},\omega}$ , we obtain from Eqs. (22) and (23):

$$\delta\vec{V}_{e\parallel\vec{k},\omega} = i \frac{\kappa_e \vec{k}_{\parallel} \delta\Phi_{\vec{k},\omega}}{B}, \quad \delta\vec{V}_{i\parallel\vec{k},\omega} = -i \frac{\kappa_i \vec{k}_{\parallel} \delta\Phi_{\vec{k},\omega}}{B}, \quad (28a)$$

$$\delta\vec{V}_{e\perp\vec{k},\omega} = -i \frac{\kappa_e [-\vec{k}_{\perp} + \kappa_e (\vec{k}_{\perp} \times \hat{b})] \delta\Phi_{\vec{k},\omega}}{(1 + \kappa_e^2) B}, \quad (28b)$$

$$\delta\vec{V}_{i\perp\vec{k},\omega} = -i \frac{\kappa_i [\vec{k}_{\perp} + \kappa_i (\vec{k}_{\perp} \times \hat{b})] \delta\Phi_{\vec{k},\omega}}{(1 + \kappa_i^2) B}. \quad (28c)$$

Writing the quasi-neutral continuity equations as

$$\partial_t n + \nabla \cdot (n \vec{V}_i) = 0, \quad \nabla \cdot (n \vec{U}) = 0, \quad (29)$$

where we neglected wave variations of ionization-recombination balance, and linearizing them with respect to density perturbations,  $\delta n_{\vec{k},\omega}$ , we obtain

$$\frac{\delta n_{\vec{k},\omega}}{n_0} = \frac{\vec{k} \cdot \delta\vec{V}_{i\vec{k},\omega}}{\Omega_{\vec{k}}^{(i)}} = -\frac{\vec{k} \cdot \delta\vec{U}_{\vec{k},\omega}}{\vec{k} \cdot \vec{U}_0}. \quad (30)$$

Here  $\Omega_{\vec{k}}^{(i)} \equiv \omega - \vec{k} \cdot \vec{V}_{i0}$  is the linear wave frequency in the ion frame;  $\delta\vec{U}_{\vec{k},\omega} = \delta\vec{V}_{e\vec{k},\omega} - \delta\vec{V}_{i\vec{k},\omega}$ , and, according to Eq. (24),

$$\vec{U}_0 = \frac{(\kappa_i + \kappa_e)[(\vec{E}_0 \times \hat{b}) - (1 + \kappa_i \kappa_e)\vec{E}_0]}{(1 + \kappa_e^2)(1 + \kappa_i^2)B}. \quad (31)$$

Using Eq. (28), we obtain

$$\vec{k} \cdot \delta\vec{V}_{i\vec{k},\omega} = -i\kappa_i \left( \frac{k_{\perp}^2}{1 + \kappa_i^2} + k_{\parallel}^2 \right) \frac{\delta\Phi_{\vec{k},\omega}}{B}, \quad (32a)$$

$$\vec{k} \cdot \delta\vec{V}_{e\vec{k},\omega} = i\kappa_e \left( \frac{k_{\perp}^2}{1 + \kappa_e^2} + k_{\parallel}^2 \right) \frac{\delta\Phi_{\vec{k},\omega}}{B}, \quad (32b)$$

so that

$$\vec{k} \cdot \delta\vec{U}_{\vec{k},\omega} = \frac{i\kappa_i \kappa_e (\kappa_e + \kappa_i) (1 + \psi_{\vec{k}}) k_{\perp}^2 \delta\Phi_{\vec{k},\omega}}{(1 + \kappa_e^2)(1 + \kappa_i^2)B}, \quad (33)$$

where

$$\psi_{\vec{k}} \equiv \psi_{\perp} \left[ 1 + (1 + \kappa_e^2)(1 + \kappa_i^2) \frac{k_{\parallel}^2}{k_{\perp}^2} \right], \quad (34a)$$

$$\psi_{\perp} \equiv \frac{1}{\kappa_i \kappa_e} = \frac{\nu_e \nu_i}{\Omega_e \Omega_i}. \quad (34b)$$

The 2-D parameter  $\psi_{\perp}$  is conventional. The newly defined 3-D parameter  $\psi_{\vec{k}}$  generalizes the traditional 3-D parameter  $\psi = \psi_{\perp}(1 + \kappa_e^2 k_{\parallel}^2/k_{\perp}^2)$  originally introduced for magnetized electrons,  $\kappa_e^2 \gg 1$ , and unmagnetized ions,  $\kappa_i^2 \ll 1$  [e.g., *Farley*, 1996]. In a more general case of  $\kappa_e^2 \gg 1$  but arbitrary  $\kappa_i$ , the parameter  $\psi_{\vec{k}}$  replaces the product  $(1 + \kappa_i^2)\psi$  [*Fejer et al.*, 1984]. In the lower ionosphere, the difference between the two is negligible,  $(1 + \kappa_i^2)\psi - \psi_{\vec{k}} = \kappa_i^2 \psi_{\perp} = \Theta_0^2 \equiv m_e \nu_e / (m_i \nu_i) \simeq 1.8 \times 10^{-4}$  [*Dimant and Milikh*, 2003; *Dimant and Oppenheim*, 2004].

Using Eqs. (32) and (33), we obtain from Eq. (30) the first-order relation between the linear fluctuations of the density and electrostatic potential,

$$\delta\Phi_{\vec{k},\omega} = i \frac{(1 + \kappa_e^2)(1 + \kappa_i^2)B(\vec{k} \cdot \vec{U}_0)}{\kappa_i \kappa_e (\kappa_e + \kappa_i) (1 + \psi_{\vec{k}}) k_{\perp}^2} \left( \frac{\delta n_{\vec{k},\omega}}{n_0} \right), \quad (35)$$

as well as the expression for the first-order wave frequency in the ion frame,

$$\Omega_{\vec{k}}^{(i)} = \frac{(1 + \kappa_e^2)[1 + (1 + \kappa_i^2)k_{\parallel}^2/k_{\perp}^2](\vec{k} \cdot \vec{U}_0)}{\kappa_e (\kappa_e + \kappa_i) (1 + \psi_{\vec{k}})}. \quad (36)$$

In the neutral frame, the corresponding frequency,  $\omega_{\vec{k}} = \Omega_{\vec{k}}^{(i)} + \vec{k} \cdot \vec{V}_{i0}$ , is

$$\omega_{\vec{k}} = \frac{(\kappa_e - \kappa_i)(\vec{k} \cdot \vec{U}_0)}{(\kappa_e + \kappa_i)(1 + \psi_{\vec{k}})} - \frac{\kappa_i \kappa_e \vec{k} \cdot (\vec{U}_0 \times \hat{b})}{\kappa_e + \kappa_i}. \quad (37)$$

When obtaining these expressions, we used the easily derived relation

$$(1 + \kappa_i \kappa_e) k_{\perp}^2 + (1 + \kappa_e^2)(1 + \kappa_i^2) k_{\parallel}^2 = \kappa_i \kappa_e k_{\perp}^2 (1 + \psi_{\vec{k}}). \quad (38)$$

As might be expected for arbitrarily magnetized electrons and ions, Eqs. (35) and (37) are symmetric with respect to the interchange between electrons and ions that requires  $\kappa_{i,e} \leftrightarrow \kappa_{e,i}$  and  $\vec{U}_0 \leftrightarrow -\vec{U}_0$ . Equation (36) for the Doppler-shifted frequency in the ion frame,  $\Omega_{\vec{k}}^{(i)}$ , is symmetric with respect to a similar expression for the wave frequency in the

electron frame,  $\Omega_{\vec{k}}^{(e)} \equiv \omega_{\vec{k}} - \vec{k} \cdot \vec{V}_{e0} = \Omega_{\vec{k}}^{(i)} - \vec{k} \cdot \vec{U}_0$ ,

$$\Omega_{\vec{k}}^{(e)} = - \frac{(1 + \kappa_i^2)[1 + (1 + \kappa_e^2)k_{\parallel}^2/k_{\perp}^2](\vec{k} \cdot \vec{U}_0)}{\kappa_i (\kappa_i + \kappa_e) (1 + \psi_{\vec{k}})}. \quad (39)$$

Notice that for prevalent waves with positive  $\vec{k} \cdot \vec{U}_0$  the shifted electron frequency  $\Omega_{\vec{k}}^{(e)}$  is always negative, while the corresponding ion frequency  $\Omega_{\vec{k}}^{(i)}$  is positive. This reflects the fact that such waves, regardless of the particle magnetization, always lag behind the streaming electrons but move ahead of the ions.

Despite the formal symmetry in the general relations between electrons and ions, their actual contributions are not equivalent. In the lower ionosphere, since  $m_i \simeq 30$  amu and  $\nu_e/\nu_i \simeq 10$  [*Kelley*, 2009], the ratio  $\kappa_e/\kappa_i$  is huge,  $\kappa_e/\kappa_i \simeq 5500$ . Then practically everywhere, except for the *D*-region altitudes below 80 km, electrons are strongly magnetized,  $\kappa_e \gg 1$ , whilst in most of the *E/D*-region electrojet ions are largely unmagnetized,  $\kappa_i \ll 1$ , reaching only a partial magnetization,  $\kappa_i \gtrsim 1$ , above 110 km. Apart from the *D*-region altitudes but practically throughout the entire electrojet, setting  $\kappa_e \gg 1$  with arbitrary  $\kappa_i$ , we reduce Eqs. (34) to (37) to simpler relations [*Fejer et al.*, 1984]:

$$\begin{aligned} \psi_{\vec{k}} &\approx \psi_{\perp} \left[ 1 + (1 + \kappa_i^2) \frac{\Omega_e^2 k_{\parallel}^2}{\nu_e^2 k_{\perp}^2} \right], \\ \omega_{\vec{k}} &\approx \frac{\vec{k} \cdot \vec{U}_0}{1 + \psi_{\vec{k}}} - \kappa_i \vec{k} \cdot (\vec{U}_0 \times \hat{b}), \end{aligned} \quad (40)$$

$$\delta\Phi_{\vec{k},\omega} = i \frac{m_i \nu_i (1 + \kappa_i^2)(\vec{k} \cdot \vec{U}_0)}{e k_{\perp}^2 (1 + \psi_{\vec{k}})} \left( \frac{\delta n_{\vec{k},\omega}}{n_0} \right).$$

For unmagnetized ions,  $\kappa_i \ll 1$ , Eq. (40) reduces further to the conventional relations [*Farley*, 1996].

Recall that all these relations represent only the first-order approximation with respect to the small parameters  $kl_i$  and  $\omega/\nu_i$ . Neglect of pressure gradients, particle inertia, etc., results in the highest-order dispersion relation for the real part of the linear wave frequency, Eq. (37). It contains no  $\pi/2$ -phase shifted corrections that determine the linear wave growth or damping. For arbitrary particle magnetization, the corresponding second-order corrections to the dispersion relation for the FB and gradient drift instabilities are obtained in the appendix of *Dimant and Oppenheim* [2011]. We should bear in mind, however, that our quasi-periodic description of the non-linearly saturated steady state requires all wave frequencies to be strictly real. This implies that the second-order destabilizing linear factors are on average balanced by non-linearities. Furthermore, non-linearly saturated turbulence itself has a strongly time-varying character caused by dynamic mode-coupling [e.g., *Hamza and St.-Maurice*, 1993a, b; *Dimant*, 2000]. All this breaks the narrowband approximation for which any wave frequency  $\omega$ , via the linear dispersion relation, is uniquely determined by the corresponding wavevector  $\vec{k}$ ,  $\omega \approx \omega_{\vec{k}}$ . This means that the  $\delta$ -function dependence of the frequency spectrum is actually spread over a finite band around  $\omega_{\vec{k}}$ . Accurate theoretical description of such non-linearly saturated states is extremely difficult, especially for strong turbulence generated by the driving field well above the instability threshold. To avoid serious difficulties and mathematical complexities, we will continue using first-order linear relations like Eqs. (28) and (35) and neglect next-order linear and non-linear corrections. We expect the corresponding errors to be reasonably small, although these expectations need additional testing.

### 3.2. Non-linear Currents

As shown in Sect. 2, the non-linear current (NC) plays an important role in energy conversion. To further clarify



its physical meaning, we calculate separately NCs for electrons and ions,  $\vec{j}_s^{\text{NC}}$  ( $s = e, i$ ), in terms of a given density-irregularity spectrum,  $\delta n_{\vec{k}, \omega}$ . These partial currents will be used in Sect. 3.3 for comparison of the partial turbulent Joule heating,  $\vec{E}_0 \cdot \vec{j}_s^{\text{NC}}$ , with the corresponding frictional heating terms.

Using Eqs. (12), (28), and (35), we obtain the partial electron NC density,  $\vec{j}_e^{\text{NC}} \equiv -e\langle\delta n\delta\vec{V}_e\rangle = -e\sum_{\vec{k}, \omega \neq 0} \delta n_{\vec{k}}^* \delta\vec{V}_{e\vec{k}}$ :

$$\vec{j}_e^{\text{NC}} = \frac{(1 + \kappa_e^2)(1 + \kappa_i^2)en_0}{\kappa_i(\kappa_e + \kappa_i)} \sum_{\vec{k}, \omega \neq 0} \frac{\vec{k} \cdot \vec{U}_0}{(1 + \psi_{\vec{k}})k_{\perp}^2} \times \left[ \vec{k}_{\parallel} + \frac{\vec{k}_{\perp} - \kappa_e(\vec{k}_{\perp} \times \hat{b})}{1 + \kappa_e^2} \right] \left| \frac{\delta n_{\vec{k}, \omega}}{n_0} \right|^2. \quad (41)$$

Similarly, we obtain the partial ion NC density,  $\vec{j}_i^{\text{NC}} \equiv e\langle\delta n\delta\vec{V}_i\rangle = e\sum_{\vec{k}, \omega \neq 0} \delta n_{\vec{k}}^* \delta\vec{V}_{i\vec{k}}$ , which differs from Eq. (41) by the replacement  $\kappa_{e,i} \leftrightarrow \kappa_{i,e}$  and the “plus” sign in front of  $(\vec{k}_{\perp} \times \hat{b})$ . The total NC,  $\vec{j}^{\text{NC}} \equiv -e\langle\delta n\delta\vec{U}\rangle = -e\sum_{\vec{k}, \omega \neq 0} \delta n_{\vec{k}}^* \delta\vec{U}_{\vec{k}}$ , is then given by

$$\vec{j}^{\text{NC}} = \vec{j}_e^{\text{NC}} + \vec{j}_i^{\text{NC}} = \frac{en_0}{\kappa_i\kappa_e} \sum_{\vec{k}, \omega \neq 0} (\vec{k} \cdot \vec{U}_0) \left| \frac{\delta n_{\vec{k}, \omega}}{n_0} \right|^2 \times \frac{(1 + \kappa_e^2)(1 + \kappa_i^2)\vec{k}_{\parallel} + (1 + \kappa_i\kappa_e)\vec{k}_{\perp} - (\kappa_e - \kappa_i)(\vec{k} \times \hat{b})}{(1 + \psi_{\vec{k}})k_{\perp}^2}. \quad (42)$$

At altitudes above 100 km, where both  $\kappa_e \gg 1 \gtrsim \kappa_i$  and  $\kappa_i\kappa_e = \psi_{\perp}^{-1} \gg 1$  hold together, according to Eq. (31), we have

$$\vec{U}_0 = \frac{\vec{E}_0 \times \hat{b} - \kappa_i \vec{E}_0}{(1 + \kappa_i^2)B}, \quad (43)$$

while the ion non-linear current turns out to be negligible compared to that of electrons,  $\vec{j}_e^{\text{NC}} \approx \vec{j}^{\text{NC}}$ . We expect no spectral asymmetry along  $\vec{B}$ , so that  $\sum_{\vec{k}, \omega \neq 0} f(k_{\perp}^2)\vec{k}_{\parallel} = 0$ . As a result, the NC density,  $\vec{j}^{\text{NC}} \perp \vec{B}$ , reduces in this limit to

$$\vec{j}^{\text{NC}} \approx -\frac{en_0}{\kappa_i} \sum_{\vec{k}, \omega \neq 0} \frac{(\vec{k} \times \hat{b})(\vec{k} \cdot \vec{U}_0)}{(1 + \psi_{\vec{k}})k_{\perp}^2} \left| \frac{\delta n_{\vec{k}, \omega}}{n_0} \right|^2. \quad (44)$$

Within the bulk electrojet where ions are unmagnetized,  $\kappa_i \ll 1$ , the  $\vec{k}$ -spectrum of irregularities is largely perpendicular to  $\vec{E}_0$ , so that  $\vec{j}^{\text{NC}}$  has there a predominantly Pedersen direction. This is of paramount importance for the global MI coupling [Dimant and Oppenheim, 2011].

### 3.3. Partial Energy Inputs and Turbulent Heating

Calculating the partial energy inputs and frictional heating sources for a specific plasma model and given turbulence spectrum allows to quantitatively understand how the turbulent energy is distributed between different plasma components. Here we obtain such expressions for arbitrarily magnetized two-fluid plasmas in the quasilinear approximation and verify, in particular, that exact Eqs. (10) and (20) remain exactly valid. The turbulent frictional heating sources found here could be included into ionosphere-thermosphere computer models, as explained in the companion paper [Dimant and Oppenheim, 2011].

Multiplying Eq. (21) by the plasma density and corresponding fluid velocities gives

$$\vec{E} \cdot \vec{j}_s = m_s \nu_s n V_s^2 \quad (45)$$

( $s = e, i$ ), where  $\vec{j}_e \equiv -en\vec{V}_e$  and  $\vec{j}_i \equiv en\vec{V}_i$  are the electron and ion partial current densities. These expressions relate the work done by the field  $\vec{E}$  on the  $s$ -particle currents to the corresponding sources of frictional heating. As mentioned in Sect. 2, the actual frictional heating of  $s$ -type particles is smaller than  $m_s \nu_{sn} n V_s^2$  because a fraction of the acquired field energy equal to  $m_s/(m_s + m_n)$  goes immediately to the colliding neutrals without heating the plasma particles [Schunk and Nagy, 2009]. This is especially true for ions with  $m_i \simeq m_n$ , whose frictional heating source is nearly half of  $m_i \nu_{in} n V_i^2$ . In what follows, we will refer to  $m_s \nu_{sn} n V_s^2$  as the  $s$ -n ‘heating term’ with the caveat that the actual  $s$ -particle frictional heating is described by  $m_n/(m_s + m_n)$  of  $m_s \nu_{sn} n V_s^2$ , while the remaining fraction goes to neutral ( $n$ ) frictional heating [Dimant and Oppenheim, 2011].

Equation (45) includes total field energy losses and plasma heating. The zero-order heating alone, i.e., that without any plasma turbulence, is described by

$$\vec{E}_0 \cdot \vec{j}_{s0} = m_s \nu_s n_0 V_{s0}^2. \quad (46)$$

Subtracting Eq. (46) from Eq. (45) and averaging yields the turbulent heating rates,

$$\vec{E}_0 \cdot \vec{j}_s^{\text{NC}} + \langle \delta \vec{E} \cdot \delta \vec{j}_s \rangle = m_s \nu_s (n_0 \langle \delta V_s^2 \rangle + 2\vec{V}_{s0} \cdot \langle \delta \vec{V}_s \delta n \rangle + \langle \delta V_s^2 \delta n \rangle), \quad (47)$$

where  $\vec{j}_e^{\text{NC}} = -e\langle\delta n\delta\vec{V}_e\rangle$  and  $\vec{j}_i^{\text{NC}} = e\langle\delta n\delta\vec{V}_i\rangle$  are the partial electron and ion contributions to the total NC given by Eq. (42). The LHS of Eq. (47) describes the additional average work by electric fields in the turbulent plasma on a given plasma species. The RHS represents the corresponding average turbulent heating per unit volume. It is not obvious, however, that the approximate quasilinear expressions obtained above ensure that the two sides of Eq. (47) are really equal. To verify the equality and clarify the physical meaning of various terms, we will calculate the two sides of Eq. (47) separately.

We start by calculating the RHS of Eq. (47) that describes the frictional heating. The positively determined and dominant term  $m_s \nu_s n_0 \langle \delta V_s^2 \rangle$  describes energization of individual plasma particles, while the other terms are associated with density variations at a given location. Consistency of the quasilinear approximation requires neglecting the last, cubically non-linear, term. To calculate average quadratically non-linear quantities in terms of given irregularity spectra, we use Eq. (12).

By using Eq. (28), for the dominant electron and ion heating terms, we obtain

$$m_s \nu_s n_0 \langle \delta V_s^2 \rangle = \frac{en_0 \kappa_s}{B} \sum_{\vec{k}, \omega \neq 0} \left( \frac{k_{\perp}^2}{1 + \kappa_s^2} + k_{\parallel}^2 \right) |\delta \Phi_{\vec{k}, \omega}|^2. \quad (48)$$

If  $\kappa_e \gg \kappa_i$  and  $\kappa_e \gg 1$  then the ion perpendicular heating dominates over the corresponding electron one, while for the parallel heating the reverse is true. At lower  $D$ -region altitudes, where electrons are partially demagnetized,  $\kappa_i \ll \kappa_e \lesssim 1$ , the electron heating always prevails. Using Eq. (35), we rewrite Eq. (48) in terms of a given density-irregularity spectrum as

$$m_e \nu_e n_0 \langle \delta V_e^2 \rangle = \frac{en_0 B (1 + \kappa_e^2) (1 + \kappa_i^2)^2}{(\kappa_e + \kappa_i)^2 \kappa_i^2 \kappa_e} \times \sum_{\vec{k}, \omega \neq 0} \frac{[1 + (1 + \kappa_e^2)k_{\parallel}^2/k_{\perp}^2](\vec{k} \cdot \vec{U}_0)^2}{(1 + \psi_{\vec{k}})^2 k_{\perp}^2} \left| \frac{\delta n_{\vec{k}, \omega}}{n_0} \right|^2 \quad (49)$$

and similar for ions with the symmetric replacement  $\kappa_{e,i} \leftrightarrow \kappa_{i,e}$ . Using Eqs. (35) and (38), for the combined heating



rate we obtain

$$\begin{aligned} & m_e \nu_e n_0 \langle \delta V_e^2 \rangle + m_i \nu_i n_0 \langle \delta V_i^2 \rangle \\ &= \frac{e B n_0 \psi_\perp (1 + \kappa_e^2)(1 + \kappa_i^2)}{\kappa_e + \kappa_i} \sum_{\vec{k}, \omega \neq 0} \frac{(\vec{k} \cdot \vec{U}_0)^2}{(1 + \psi_{\vec{k}}) k_\perp^2} \left| \frac{\delta n_{\vec{k}, \omega}}{n_0} \right|^2 \end{aligned} \quad (50a)$$

$$= \frac{e n_0 (\kappa_i + \kappa_e)}{B \psi_\perp (1 + \kappa_e^2)(1 + \kappa_i^2)} \sum_{\vec{k}, \omega \neq 0} (1 + \psi_{\vec{k}}) k_\perp^2 \left| \delta \Phi_{\vec{k}, \omega} \right|^2. \quad (50b)$$

Equation (50), presented here in terms of both  $\delta n_{\vec{k}, \omega}$  and  $\delta \Phi_{\vec{k}, \omega}$ , allows one to understand the quantitative difference between 2-D and 3-D turbulent heating. The 3-D effect of parallel-field dominated turbulent heating [Dimant and Milikh, 2003; Milikh and Dimant, 2003] is entirely due to the difference between  $\psi_{\vec{k}}$  and  $\psi_\perp$  in the multipliers  $(1 + \psi_{\vec{k}})$ . While the total perpendicular turbulent heating is described by the  $(1 + \psi_\perp)$  component, the total parallel turbulent heating derives from the remainder,  $\psi_{\vec{k}} - \psi_\perp = \psi_\perp (1 + \kappa_e^2)(1 + \kappa_i^2) k_\parallel^2 / k_\perp^2$ , as seen from Eq. (34). If  $|\delta n_{\vec{k}, \omega}|^2$  were equal in 2-D and 3-D then, according to Eq. (50a), larger  $(1 + \psi_{\vec{k}})$  would reduce total turbulent heating in 3-D compared to 2-D. We have, however, the reverse by the following reason. Heuristic arguments require the perpendicular rms turbulent fields  $\sim \sum_{\vec{k}, \omega \neq 0} k_\perp^2 |\delta \Phi_{\vec{k}, \omega}|^2$  to be approximately equal in 2-D and 3-D [Dimant and Milikh, 2003; Dimant and Oppenheim, 2011]. According to Eq. (50b), this leads to stronger heating in 3-D compared to 2-D, entirely due to larger density perturbations,  $\sum_{\vec{k}, \omega \neq 0} |\delta n_{\vec{k}, \omega}|^2 \propto \sum_{\vec{k}, \omega \neq 0} (1 + \psi_{\vec{k}})^2 k_\perp^2 |\delta \Phi_{\vec{k}, \omega}|^2$ . The same pertains to the non-linear currents discussed in Sect. 3.2. All these heuristic inferences have been confirmed by our recent supercomputer PIC simulations [Oppenheim et al., 2011].

The second term in the RHS of Eq. (47), calculated by expressing  $\delta \vec{V}_{e,i}$  and  $\vec{V}_{e,i0}$  in terms of  $\delta \vec{U}$  and  $\vec{U}_0$ , using Eq. (27), and  $\vec{U}_0 \times \hat{b}$  in terms of  $\vec{E}_0$ , using Eq. (25), is

$$\begin{aligned} & 2m_i (\nu_i \vec{V}_{i0} \cdot \langle \delta n \delta \vec{V}_i \rangle) \\ &= \frac{2e n_0 (1 + \kappa_e^2)}{\kappa_e (\kappa_i + \kappa_e)} \sum_{\vec{k}, \omega \neq 0} \frac{(\vec{k} \cdot \vec{E}_0)(\vec{k} \cdot \vec{U}_0)}{(1 + \psi_{\vec{k}}) k_\perp^2} \left| \frac{\delta n_{\vec{k}, \omega}}{n_0} \right|^2 \end{aligned} \quad (51)$$

and similar for electrons, with the symmetric replacement  $\kappa_{e,i} \leftrightarrow \kappa_{i,e}$ . At higher altitudes, where  $\psi_\perp = (\kappa_e \kappa_i)^{-1} < 1$  and  $\kappa_e \gg 1$ , the ion component dominates over the electron component, while at lower altitudes,  $\psi_\perp > 1$ , the reverse holds. Adding up the two plasma components gives

$$\begin{aligned} & 2m_i \nu_i (\vec{V}_{i0} \cdot \langle \delta n \delta \vec{V}_i \rangle) + 2m_e \nu_e (\vec{V}_{e0} \cdot \langle \delta n \delta \vec{V}_e \rangle) \\ &= 2e n_0 (1 + \psi_\perp) \sum_{\vec{k}, \omega \neq 0} \frac{(\vec{k} \cdot \vec{E}_0)(\vec{k} \cdot \vec{U}_0)}{(1 + \psi_{\vec{k}}) k_\perp^2} \left| \frac{\delta n_{\vec{k}, \omega}}{n_0} \right|^2. \end{aligned} \quad (52)$$

In the most of electrojet, these terms are small compared to those in Eq. (50), although at the top of the electrojet they can become comparable.

To verify that general Eqs. (10) and (20) exactly hold in our quasilinear calculations, now we proceed to calculating the LHS of Eq. (47). Each of the electron and ion terms,  $\langle \delta \vec{E} \cdot \delta \vec{j}_{e,i} \rangle$ , can be separated into two distinct parts,

$$\langle \delta \vec{E} \cdot \delta \vec{j}_s \rangle = \langle \delta \vec{E} \cdot \delta \vec{j}_s \rangle_1 + \langle \delta \vec{E} \cdot \delta \vec{j}_s \rangle_2, \quad (53)$$

where  $\langle \delta \vec{E} \cdot \delta \vec{j}_s \rangle_1 \equiv -e n_0 \langle \delta \vec{V}_s \cdot \delta \vec{E} \rangle$ ,  $\langle \delta \vec{E} \cdot \delta \vec{j}_s \rangle_2 \equiv -e \vec{V}_{e0} \cdot \langle \delta n \delta \vec{E} \rangle$ , and we neglect the cubically non-linear corrections,  $e \langle \delta n \delta \vec{V}_s \cdot \delta \vec{E} \rangle$ . Using Eqs. (25) and (28), we find that the first

term,  $\langle \delta \vec{E} \cdot \delta \vec{j}_s \rangle_1$ , equals the fixed-density frictional heating rate,

$$\langle \delta \vec{E} \cdot \delta \vec{j}_s \rangle_1 = m_s \nu_s n_0 \langle \delta V_s^2 \rangle, \quad (54)$$

while the combination of the electron and ion second terms in Eq. (53) yields

$$\begin{aligned} & \langle \delta \vec{E} \cdot \delta \vec{j}_e \rangle_2 + \langle \delta \vec{E} \cdot \delta \vec{j}_i \rangle_2 \equiv \langle \delta \vec{E} \cdot \delta \vec{j} \rangle_2 \\ &= - \frac{e B n_0 (1 + \kappa_e^2)(1 + \kappa_i^2) \psi_\perp}{(\kappa_e + \kappa_i)} \sum_{\vec{k}, \omega \neq 0} \frac{(\vec{k} \cdot \vec{U}_0)^2}{(1 + \psi_{\vec{k}}) k_\perp^2} \left| \frac{\delta n_{\vec{k}}}{n_0} \right|^2 \end{aligned} \quad (55)$$

By combining Eqs. (50) and (53)–(55), we verify that, in accord with Eq. (10),  $\langle \delta \vec{E} \cdot \delta \vec{j} \rangle = 0$ . Due to this, turbulent Joule heating,  $L_{\text{turb}} \equiv \langle \vec{E} \cdot \vec{j} \rangle - \vec{E}_0 \cdot \vec{j}_0 = \vec{E}_0 \cdot \vec{j}^{\text{NC}} + \langle \delta \vec{E} \cdot \delta \vec{j} \rangle$ , in accord with Eq. (20), equals the total average work of the external electric field on the total non-linear current,  $P_{\text{NC}} \equiv \vec{E}_0 \cdot \vec{j}^{\text{NC}}$ . This quantity, in turn, should equal the total frictional heating source given by combining the RHS of Eq. (47) for all plasma species. Indeed, using Eq. (42) for  $\vec{j}^{\text{NC}}$ , we obtain

$$\begin{aligned} P_{\text{NC}} &= \frac{e B n_0 \psi_\perp (1 + \kappa_e^2)(1 + \kappa_i^2)}{\kappa_e + \kappa_i} \sum_{\vec{k}, \omega \neq 0} \frac{(\vec{k} \cdot \vec{U}_0)^2}{(1 + \psi_{\vec{k}}) k_\perp^2} \left| \frac{\delta n_{\vec{k}}}{n_0} \right|^2 \\ &+ 2(1 + \psi_\perp) e n_0 \sum_{\vec{k}, \omega \neq 0} \frac{(\vec{k} \cdot \vec{E}_0)(\vec{k} \cdot \vec{U}_0)}{(1 + \psi_{\vec{k}}) k_\perp^2} \left| \frac{\delta n_{\vec{k}}}{n_0} \right|^2, \end{aligned} \quad (56)$$

which equals the total turbulent heating found by combining Eqs. (50) and (52).

Thus, our fluid-model calculations for arbitrarily magnetized plasma particles in the quasilinear approximation have fully confirmed the exact general relations derived in Sect. 2 exclusively from Maxwell's equations. The partial relations for various energy conversion terms show how the deposited field energy is divided between the electron and ion heating channels and allow one to properly interpret the corresponding terms.

## 4. Global Energy Flow

Now we discuss how the energy from the Earth's magnetosphere is deposited to the  $E/D$ -region electrojet. From the above treatment it is clear that the global energy flow should be analyzed based on the total average currents that include the NCs. To obtain energy balance equations similar to Eqs. (2) for spatially and temporally averaged fields introduced in Eq. (7), we use separate linear Maxwell's equations for the average fields and for disturbances caused by the total average currents,  $\langle \vec{j} \rangle = \vec{j}^{\text{tot}} \equiv \vec{j}_0 + \vec{j}_{\text{NL}}$ , as we did in deriving Eq. (9) for the wave perturbations. As a result, ignoring the induction component of  $\langle \vec{E} \rangle = \vec{E}_0$ , i.e., assuming  $\nabla_{\vec{r}} \times \vec{E}_0 = 0$ , we obtain

$$\partial_\tau \left[ \frac{\epsilon_0 (E_0^2 + c^2 \langle B \rangle^2)}{2} \right] + \nabla_{\vec{r}} \cdot \Delta \vec{S} = -\vec{E}_0 \cdot \vec{j}^{\text{tot}}, \quad (57)$$

where  $\tau, \vec{r}$  are the large-scale variables introduced in Sect. 2, and

$$\Delta \vec{S} \equiv \frac{\vec{E}_0 \times \Delta \vec{B}}{\mu_0} = \epsilon_0 c^2 \vec{E}_0 \times \Delta \vec{B}. \quad (58)$$

Here  $\Delta \vec{B} \equiv \langle \vec{B} \rangle - \vec{B}_0$  is the quasi-stationary large-scale magnetic field disturbance, where by  $\vec{B}_0$  we mean the geomagnetic field undisturbed by the electrojets,  $\nabla_{\vec{r}} \times \vec{B}_0 = 0$ , so that  $\nabla_{\vec{r}} \cdot (\vec{E}_0 \times \vec{B}_0) = 0$ . The disturbance  $\Delta \vec{B}$  is caused by

the total average electrojet currents,  $\nabla \times \Delta \vec{B} \approx \mu_0 \vec{j}^{\text{tot}}$ . It is usually so small,  $|\Delta \vec{B}| \lesssim 10^{-3} B_0$ , that can be neglected in the expression for the magnetic energy density,  $\langle B \rangle^2 \approx B_0^2$ . However,  $\Delta \vec{B}$  is crucial for the Poynting flux  $\Delta \vec{S}$  that provides a downward flow of field energy from the magnetosphere to the  $E/D$ -region ionosphere. Further, bearing in mind that  $\vec{j}^{\text{tot}} = \vec{\sigma}^{\text{tot}} \cdot \vec{E}_0$ , the work of the external field on the total current in the RHS of Eq. (57) can be written as  $\vec{E}_0 \cdot \vec{j}^{\text{tot}} = \sigma_P^{\text{tot}} E_0^2$ , where  $\vec{\sigma}^{\text{tot}}$  and  $\sigma_P^{\text{tot}}$  are the total conductivity tensor and Pedersen conductivity, respectively [Dimant and Oppenheim, 2011]. In the turbulent electrojet, the quantity  $\sigma_P^{\text{tot}} E_0^2$  represents the combined laminar and turbulent Joule heating. Bearing in mind quasi-stationary conditions, from Eq. (57) we estimate the magnitude of the Poynting flux on top of the electrojet as  $|\Delta \vec{S}| \sim \sigma_P^{\text{tot}} E_0^2 L_{\parallel}$ , where  $L_{\parallel}$  is the characteristic size of the electrojet along the nearly vertical magnetic field. The corresponding disturbance of the magnetic field,  $\Delta \vec{B}$ , has a significant component perpendicular to both  $\vec{E}_0$  and  $\vec{B}_0$  with the magnitude  $\sim \mu_0 \sigma_P^{\text{tot}} E_0 L_{\parallel}$ .

Now we do the same for the plasma. Averaging Eq. (5) over small turbulent scales and neglecting  $\langle \delta \vec{E} \cdot \delta \vec{j} \rangle$ , in accord with the analysis of Sect. 2, we obtain

$$\partial_t \sum_s \langle \mathcal{E}_s \rangle + \nabla_r \cdot \sum_s \langle \vec{K}_s \rangle = \vec{E}_0 \cdot \vec{j}^{\text{tot}} + \sum_s \langle L_s \rangle. \quad (59)$$

While the RHS of Eq. (57) has only one term describing the total field energy loss to charged particles, the RHS of Eq. (59) has two terms. The first term,  $\vec{E}_0 \cdot \vec{j}^{\text{tot}} = \sigma_P^{\text{tot}} E_0^2$ , describes the total Joule heating rate due to the total energy input from the fields. The second term describes particle energy dissipation in the abundant neutral atmosphere. For particle fluxes dominated by the thermal bulk, the two terms almost cancel each other locally, so that the flux divergence term  $\nabla_r \cdot \sum_s \langle \vec{K}_s \rangle$  is expected to be much less than  $\nabla_r \cdot \Delta \vec{S}$  in Eq. (57). This means that the energy transport of ionospheric particles should be much weaker than that of fields. The reason why the particle energy transport plays a minor role is associated with relatively short mean electron and ion free paths, even in the almost vertical direction along  $\vec{B}_0$ . We should bear in mind, however, that the fluxes  $\langle \vec{K}_s \rangle$  can also include high-energy precipitating particles that may comprise a significant part of the field-aligned (Birkeland) currents within auroral arcs. These occasions may break the nearly perfect local balance between the Joule heating and atmospheric cooling. Although in these cases  $|\nabla_r \cdot \sum_s \langle \vec{K}_s \rangle|$  should still remain less than  $|\nabla_r \cdot \Delta \vec{S}|$ , the two fluxes may be closer to each other than those for the nearly local thermal-bulk dominated balance.

Now we compare the total field and particle fluxes along the nearly vertical magnetic field in greater detail. We can estimate the particle energy flux magnitude as  $|\sum_s \langle \vec{K}_s \rangle| \sim \langle \mathcal{E} \rangle j_{\parallel}$ , where  $\langle \mathcal{E} \rangle$  is an effective energy of charged particles. Using the charge flow conservation,  $\nabla \cdot \vec{j} = 0$ , we estimate the parallel current density as  $j_{\parallel} \sim L_{\parallel} \sigma_P E_0 / L_P$ , where  $L_P$  is the characteristic scale of current density variations in the Pedersen direction. As a result, we have  $|\sum_s \langle \vec{K}_s \rangle| / |\Delta \vec{S}| \sim \langle \mathcal{E} \rangle / (e |\Delta \Phi|)$ , where  $\Delta \Phi \sim L_P E_0$  is the characteristic cross-polar cap potential. Typical values of  $\Delta \Phi$  are  $\sim 100$  kV. If this current is mainly provided by thermal bulk particles then their energy is many orders of magnitude smaller,  $\langle \mathcal{E} \rangle \lesssim 1$  eV. Precipitating particles can have a rather high energy,  $\langle \mathcal{E} \rangle \lesssim 30$  keV [e.g., Ashrafi et al., 2005], so that the particle energy flux can sometimes be comparable to the Poynting flux.

Buchert et al. [2006] in their analysis of global energy flow between the magnetosphere and  $E$ -region ionosphere put

more stress on the Birkeland currents. These field-aligned currents are important for charge conservation and they provide the MI coupling via particle precipitation. Furthermore, electron fluxes along  $\vec{B}_0$ , because of their high parallel mobility, ensure effective mapping of the electric field from the magnetosphere to lower ionosphere. From the energy transport viewpoint, however, our analysis gives preference to the Poynting flux. It is interesting to note that 2-D or 3-D simulations of the  $E/D$ -region instabilities in purely periodic boxes have always generated the DC currents  $\vec{j}^{\text{tot}}$  in a plane perpendicular to  $\vec{B}_0$ . According to Maxwell's equations,  $\vec{j}^{\text{tot}}$  must generate quasi-stationary loop-like magnetic disturbances  $\Delta \vec{B}$ , which in the employed electrostatic codes are ignored by definition. Furthermore, such  $\Delta \vec{B}$  would even violate the imposed periodicity, unless one presumes on the 3-D box boundaries surface currents that exactly balance the volumetric currents. If, however, one did not ignore  $\Delta \vec{B}$  then the corresponding Poynting flux,  $c^2 \epsilon_0 \vec{E}_0 \times \Delta \vec{B}$ , would be directed inward the box and provide the required energy input.

## 5. Summary and Conclusions

Plasma turbulence generated by  $E/D$ -region instabilities can contribute significantly to the global energy exchange between the magnetosphere and ionosphere. The spatially-temporally averaged energy deposit in the turbulent electrojet is given by  $\vec{E}_0 \cdot \vec{j}^{\text{tot}}$ , where the total current density  $\vec{j}^{\text{tot}}$ , in addition to the regular current density,  $\vec{j}_0 = \vec{\sigma}_P^0 \cdot \vec{E}_0$ , includes the non-linear current (NC) density,  $\vec{j}^{\text{NC}}$ , caused by low-altitude plasma turbulence [Rogister and Jamin, 1975; Oppenheim, 1997]. The work of the external field on the NC,  $\vec{E}_0 \cdot \vec{j}^{\text{NC}}$ , provides the required energy input for anomalous (turbulent) heating of both electrons and ions [Buchert et al., 2006]. In Sect. 2 we prove this earlier conjecture using first principles with virtually no approximations. Specific fluid-model calculations for arbitrarily magnetized plasma in the quasilinear approximation show how exactly the deposited field energy is distributed between electrons and ions. This yields explicit NC expressions given by Eq. (42), and turbulent sources of anomalous electron and ion heating given by Eq. (49). It has been known for a long time that anomalous electron heating (AEH) is largely a 3-D effect caused by turbulent electric fields parallel to  $\vec{B}$  [St.-Maurice and Laher, 1985; Providakes et al., 1988; Dimant and Milikh, 2003; Bahcivan et al., 2006]. According to the new development, this requires significantly larger  $\vec{E}_0 \cdot \vec{j}^{\text{NC}}$  in 3-D than in 2-D. Due to the mirror symmetry along  $\vec{B}$ , neither  $\vec{E}_0$  nor  $\vec{j}^{\text{NC}}$  have any significant components in the  $\vec{B}$  direction. The difference in  $\vec{E}_0 \cdot \vec{j}^{\text{NC}}$  between the 3-D and 2-D is entirely due to noticeably larger 3-D NC caused by larger density perturbations, as explained in the text below Eq. (50). This prediction has been confirmed by our recent 2-D and 3-D PIC simulations [Oppenheim et al., 2011]. As discussed in the companion paper [Dimant and Oppenheim, 2011], a strong NC, either by itself or combined with AEH [Milikh and Dimant, 2003; Milikh et al., 2006], can significantly increase the global ionospheric conductances. This may have serious implications for predictive modeling of MI coupling and space weather.

## Appendix: Validation of Electrostatic Approximation

Using some relations obtained in Sect. 2, we now discuss the validity of the electrostatic approximation in describing wave processes in the lower ionosphere. To the best of our knowledge, the electrostatic approximation for the  $E$ -region

instabilities has always been employed but no detailed analysis of its validity been done, especially for the general span of magnetization conditions considered in this paper. There are occasions when induction fields in the ionosphere play an important role [e.g., *Amm et al.*, 2008; *Vanhamäki et al.*, 2007]. The main reason why one might question the validity of electrostatic approximation in the description of  $E/D$ -region wave processes is that even tiny induction corrections to the wave electric field along  $\vec{B}$  could modify the small parallel turbulent electric field largely responsible for AEH.

To estimate a possible non-electrostatic component of a separate wave field harmonic,  $\delta\vec{E}_{\vec{k},\omega}$ , we split it into the electrostatic (curl-free) part,  $\delta\vec{E}_{\vec{k},\omega}^{\text{ES}} \equiv (\vec{k} \cdot \delta\vec{E}_{\vec{k},\omega})\vec{k}/k^2$ , and the induction part,  $\delta\vec{E}_{\vec{k},\omega}^{\text{IND}} \equiv \delta\vec{E}_{\vec{k},\omega} - \delta\vec{E}_{\vec{k},\omega}^{\text{ES}} = -\vec{k} \times (\vec{k} \times \delta\vec{E}_{\vec{k},\omega})/k^2$ . Then Eq. (15) yields

$$\delta\vec{E}_{\vec{k},\omega}^{\text{ES}} = -\frac{i(\vec{k} \cdot \delta\vec{j}_{\vec{k},\omega})\vec{k}}{\varepsilon_0\omega k^2}, \quad (60a)$$

$$\delta\vec{E}_{\vec{k},\omega}^{\text{IND}} = -\frac{i\omega\vec{k} \times (\vec{k} \times \delta\vec{j}_{\vec{k},\omega})}{\varepsilon_0(k^2 c^2 - \omega^2)k^2}. \quad (60b)$$

The wave current density,  $\delta\vec{j}_{\vec{k},\omega}$ , is determined by an anisotropic response to the total turbulent electric field,  $\delta\vec{E}_{\vec{k},\omega}$ . Even if the turbulent field is largely electrostatic,  $\delta\vec{E}_{\vec{k},\omega} \simeq \delta\vec{E}_{\vec{k},\omega}^{\text{ES}} \parallel \vec{k}$ , this anisotropy can give rise to a non-negligible component of  $\delta\vec{j}_{\vec{k},\omega}$  which is not parallel to  $\vec{k}$ . According to Eq. (60b), this component generates non-zero  $\vec{k} \times (\vec{k} \times \delta\vec{j}_{\vec{k},\omega}) = \vec{k}(\vec{k} \cdot \delta\vec{j}_{\vec{k},\omega}) - k^2\delta\vec{j}_{\vec{k},\omega}$ , i.e., finite  $\delta\vec{E}_{\vec{k},\omega}^{\text{IND}}$ .

Using a perturbation technique in which the zero-order wave field is electrostatic,  $\delta\vec{E}_{\vec{k},\omega} \approx \delta\vec{E}_{\vec{k},\omega}^{\text{ES}} = -i\vec{k}\delta\Phi_{\vec{k},\omega}$ , one can easily estimate the next-order induction component,  $\delta\vec{E}_{\vec{k},\omega}^{\text{IND}}$ . Considering the wave with  $\vec{k}$  in the  $x, z$ -plane ( $\hat{z} \parallel \vec{B}_0$ ), neglecting density perturbations, and applying to  $\delta\vec{E}_{\vec{k},\omega}$  the regular linear conductivity, we obtain

$$\delta\vec{j}_{\vec{k},\omega} \approx \overleftrightarrow{\sigma}^0 \cdot \delta\vec{E}_{\vec{k},\omega}^{\text{ES}} = -i(\overleftrightarrow{\sigma}^0 \cdot \vec{k})\delta\Phi_{\vec{k},\omega} = -i\delta\Phi_{\vec{k},\omega} \begin{bmatrix} \sigma_P^0 k_{\perp} \\ -\sigma_H^0 k_{\perp} \\ \sigma_{\parallel}^0 k_{\parallel} \end{bmatrix},$$

where we have restricted ourselves to the regular conductivity tensor  $\overleftrightarrow{\sigma}^0$  [Kelley, 2009],

$$\sigma_{\parallel}^0 \equiv \frac{\vec{j}_{0\parallel} \cdot \vec{E}_{0\parallel}}{E_{0\parallel}^2} = \frac{(\kappa_e + \kappa_i)ne}{B}, \quad (61a)$$

$$\sigma_P^0 \equiv \frac{\vec{j}_{0\perp} \cdot \vec{E}_{0\perp}}{E_{\perp}^2} = \frac{(\kappa_e + \kappa_i)(1 + \kappa_i\kappa_e)ne}{(1 + \kappa_e^2)(1 + \kappa_i^2)B}, \quad (61b)$$

$$\sigma_H^0 \equiv \frac{\vec{j}_{0\perp} \cdot (\vec{E}_0 \times \hat{b})}{E_{0\perp}^2} = -\frac{(\kappa_e^2 - \kappa_i^2)ne}{(1 + \kappa_e^2)(1 + \kappa_i^2)B}. \quad (61c)$$

Since the anomalous conductivity discussed in the companion paper is of the same order of magnitude at most, then according to Eq. (60) we obtain

$$\delta\vec{E}_{\vec{k},\omega}^{\text{ES}} \simeq -\frac{(\sigma_P^0 + \sigma_{\parallel}^0 k_{\parallel}^2/k_{\perp}^2)\delta\Phi_{\vec{k},\omega}}{\varepsilon_0\omega} \begin{bmatrix} k_{\perp} \\ 0 \\ k_{\parallel} \end{bmatrix}, \quad (62)$$

$$\delta\vec{E}_{\vec{k},\omega}^{\text{IND}} \simeq -\frac{\omega\delta\Phi_{\vec{k},\omega}}{\varepsilon_0 k^2 c^2} \begin{bmatrix} -\sigma_{\parallel}^0 k_{\parallel} \\ -\sigma_H^0 k_{\perp} \\ \sigma_{\parallel}^0 k_{\parallel} \end{bmatrix}, \quad (63)$$

where we have neglected  $\sigma_P^0$  compared to  $\sigma_{\parallel}^0$  and  $k_{\parallel}^2$  compared to  $k_{\perp}^2 \approx k^2$ . We also have taken into account that in  $E/D$ -region processes the wave phase speed,  $V_{\text{ph}} = \omega/k$ , is many orders of magnitude less than the speed of light, so that  $\omega^2$  in the denominator of Eq. (60b) can always be neglected compared to  $k^2 c^2$ .

Comparing Eqs. (62) and (63) for both parallel and perpendicular to  $\vec{B}_0$  components and presuming  $\sigma_{\parallel}^0 k_{\parallel}^2/k_{\perp}^2 \lesssim \sigma_P^0$ , we see that the smallness of  $|\delta\vec{E}_{\vec{k},\omega}^{\text{IND}}/\delta\vec{E}_{\vec{k},\omega}^{\text{ES}}|$  is ensured by

$$\frac{V_{\text{ph}}}{c} \ll \left(\frac{\sigma_P^0}{\sigma_{\parallel}^0}\right)^{1/2}, \quad \frac{V_{\text{ph}}}{c} \ll \left(\frac{\sigma_P^0}{\sigma_H^0}\right)^{1/2}. \quad (64)$$

The first inequality pertains to the parallel components of the turbulent electric field,  $\delta\vec{E}_{\vec{k},\omega\parallel}$ , while the second, less restrictive, inequality pertains to the corresponding perpendicular components,  $\delta\vec{E}_{\vec{k},\omega\perp}$ . As mentioned above, breaking of the parallel-field condition may be of importance because  $\delta\vec{E}_{\vec{k},\omega\parallel}$  is crucial for AEH. For magnetized electrons, up to the top electrojet where  $\kappa_e \gg 1$  and  $\kappa_i \sim 1$ , we have  $\sigma_P^0 \sim \kappa_i ne/B$ ,  $\sigma_H^0 \sim ne/B$ ,  $\sigma_{\parallel}^0 \approx \kappa_e ne/B$ , so that the most restrictive first inequality becomes

$$\frac{V_{\text{ph}}}{c} \ll \left(\frac{\kappa_i}{\kappa_e}\right)^{1/2} = \Theta_0 \simeq 1.4 \times 10^{-2}. \quad (65)$$

Even for an extremely strong convection electric field of  $E_0 \simeq 150$  mV/m, the wave phase velocity may reach 3 km/s at most,  $V_{\text{ph}}/c \simeq 10^{-5}$ , so that this condition holds with a big reserve. Thus for typical  $E/D$ -region wave processes the electrostatic approximation is always valid even for small parallel electric-field components,  $\delta\vec{E}_{\vec{k},\omega\parallel}$ .

**Acknowledgments.** This work was supported by National Science Foundation Ionospheric Physics Grants No. ATM-0442075 and ATM-0819914.

## References

- Amm, O., A. Aruliah, S. C. Buchert, R. Fujii, J. W. Gjerloev, A. Ieda, T. Matsuo, C. Stolle, H. Vanhamäki, and A. Yoshikawa (2008), Towards understanding the electrodynamics of the 3-dimensional high-latitude ionosphere: present and future, *Ann. Geophys.*, *26*, 3913–3932, doi:10.5194/angeo-26-3913-2008.
- Ashrafi, M., M. J. Kosch, and F. Honary (2005), Comparison of the characteristic energy of precipitating electrons derived from ground-based and DMSP satellite data, *Ann. Geophys.*, *23*, 135–145, doi:10.5194/angeo-23-135-2005.
- Bahcivan, H. (2007), Plasma wave heating during extreme electric fields in the high-latitude E region, *Geophys. Res. Lett.*, *34*, L15106, doi:10.1029/2006GL029236.
- Bahcivan, H., R. B. Cosgrove, and R. T. Tsunoda (2006), Parallel electron streaming in the high-latitude E region and its effect on the incoherent scatter spectrum, *J. Geophys. Res.*, *111*, A07306, doi:10.1029/2005JA011595.
- Balsley, B. B., and D. T. Farley (1971), Radar studies of the equatorial electrojet at three frequencies, *J. Geophys. Res.*, *76*, 8341–8351.
- Buchert, S. C., T. Hagfors, and J. F. McKenzie (2006), Effect of electrojet irregularities on DC current flow, *J. Geophys. Res.*, *111*, A02305, doi:10.1029/2004JA010788.
- Buneman, O. (1963), Excitation of field aligned sound waves by electron streams, *Phys. Rev. Lett.*, *10*, 285–288.
- Cohen, R., and K. L. Bowles (1967), Secondary irregularities in the equatorial electrojet, *J. Geophys. Res.*, *72*, 885–894.
- Crochet, M., C. Hanuise, and P. Broche (1979), HF radar studies of two-stream instability during an equatorial counter electrojet, *J. Geophys. Res.*, *84*, 5223–5233.
- D'Angelo, N., H. L. Pecseli, and P. I. Petersen (1974), The Farley instability - A laboratory test, *J. Geophys. Res.*, *79*, 4747–4751, doi:10.1029/JA079i031p04747.

- Dimant, Y. S. (2000), Nonlinearly saturated dynamical state of a three-wave mode-coupled dissipative system with linear instability, *Phys. Rev. Lett.*, *84*, 622–625.
- Dimant, Y. S., and G. M. Milikh (2003), Model of anomalous electron heating in the E region: 1. Basic theory, *J. Geophys. Res.*, *108*, 1350, doi:10.1029/2002JA009524.
- Dimant, Y. S., and M. M. Oppenheim (2004), Ion thermal effects on E-region instabilities: linear theory, *J. Atmos. Terr. Phys.*, *66*, 1639–1654.
- Dimant, Y. S., and M. M. Oppenheim (2011), Magnetosphere-ionosphere coupling through E-region turbulence: anomalous conductivity and frictional heating, *J. Geophys. Res.*
- Dimant, Y. S., and R. N. Sudan (1995), Kinetic theory of the Farley-Buneman instability in the E region of the ionosphere, *J. Geophys. Res.*, *100*, 14,605–14,624.
- Dimant, Y. S., and R. N. Sudan (1997), Physical nature of a new cross-field current-driven instability in the lower ionosphere, *J. Geophys. Res.*, *102*, 2551–2564, doi:10.1029/96JA03274.
- Farley, D. T. (1963), A plasma instability resulting in field-aligned irregularities in the ionosphere, *J. Geophys. Res.*, *68*, 6083–6097.
- Farley, D. T. (1996), Theories of auroral electrojet instabilities, in *Plasma Instabilities in the Ionospheric E-Region*, edited by K. Schlegel, p. 119, Proceedings of a special workshop on E-region plasma instabilities held at the MPI für Aeronomie, Lindau, Germany, October 1995, Cuvillier Verlag, Göttingen, Germany.
- Fejer, B. G., J. Providakes, and D. T. Farley (1984), Theory of plasma waves in the auroral E region, *J. Geophys. Res.*, *89*, 7487–7494.
- Fontenla, J. M., W. K. Peterson, and J. Harder (2008), Chromospheric heating by the Farley-Buneman instability, *Astron. Astrophys.*, *480*, 839–846, doi:10.1051/0004-6361:20078517.
- Foster, J. C., and P. J. Erickson (2000), Simultaneous observations of E-region coherent backscatter and electric field amplitude at F-region heights with the Millstone Hill UHF radar, *Geophys. Res. Lett.*, *27*, 3177–3180.
- Fukao, S., M. Yamamoto, R. T. Tsunoda, H. Hayakawa, and T. Mukai (1998), The SEEK (Sporadic-E Experiment over Kyushu) campaign, *Geophys. Res. Lett.*, *25*, 1761–1764.
- Gogoberidze, G., Y. Voitenko, S. Poedts, and M. Goossens (2009), Farley-Buneman Instability in the Solar Chromosphere, *Astrophys. J.*, *706*, L12–L16, doi:10.1088/0004-637X/706/1/L12.
- Guild, T. B., H. E. Spence, E. L. Kepko, V. G. Merkin, J. G. Lyon, M. J. Wiltberger, and C. C. Goodrich (2008), Geotail and LFM comparisons of plasma sheet climatology 1: Average values, *J. Geophys. Res.*, *113*(A04216), doi:10.1029/2007JA012611.
- Gurevich, A. V. (1978), *Nonlinear phenomena in the ionosphere*, Springer-Verlag, New York.
- Hamza, A. M., and J.-P. St.-Maurice (1993a), A turbulent theoretical framework for the study of current-driven E region irregularities at high latitudes: basic derivation and application to gradient-free situations, *J. Geophys. Res.*, *98*, 11,587–11,599.
- Hamza, A. M., and J.-P. St.-Maurice (1993b), A self-consistent full turbulent theory of radar auroral backscatter, *J. Geophys. Res.*, *98*, 11,601–11,613.
- Hoh, F. C. (1963), Instability of penning-type discharge, *Phys. Fluids*, *6*, 1184.
- John, P. I., and Y. C. Saxena (1975), Observation of the Farley-Buneman instability in laboratory plasma, *Geophys. Res. Lett.*, *2*, 251–254, doi:10.1029/GL002i006p00251.
- Kagan, L. M., and M. C. Kelley (2000), A thermal mechanism for generation of small-scale irregularities in the ionospheric E region, *J. Geophys. Res.*, *105*(A3), 5291–5302.
- Kelley, M. C. (2009), *The Earth's Ionosphere: Plasma physics and Electrodynamics*, Academic Press, Amsterdam.
- Koepke, M. E. (2008), Interrelated laboratory and space plasma experiments, *Reviews of Geophysics*, *46*, RG3001, doi:10.1029/2005RG000168.
- Kudeki, E., B. G. Fejer, D. T. Farley, and C. Hanuise (1987), The CONDOR equatorial electrojet campaign: Radar results, *J. Geophys. Res.*, *92*, 13,561–13,577.
- Landau, L. D., and E. M. Lifshitz (2000), *Statistical Physics, Third Edition: Part 1 (Course of Theoretical Physics, Vol. 5)*, Butterworth-Heinemann.
- Liperovsky, V. A., C. Meister, E. V. Liperovskaya, K. V. Popov, and S. A. Senchenkov (2000), On the generation of modified low-frequency Farley-Buneman waves in the solar atmosphere, *Astronomische Nachrichten*, *321*, 129–136, doi:10.1002/(SICI)1521-3994(200005)321:2<129::AID-ASNA129>3.0.CO;2-2.
- Maeda, K., T. Tsuda, and H. Maeda (1963), Theoretical interpretation of the equatorial sporadic E layers, *Phys. Rev. Lett.*, *11*, 406–409.
- Merkin, V. G., A. S. Sharma, K. Papadopoulos, G. Milikh, J. Lyon, and C. Goodrich (2005a), Global MHD simulations of the strongly driven magnetosphere: Modeling of the transpolar potential saturation, *J. Geophys. Res.*, *110*, A09203, doi:10.1029/2004JA010993.
- Merkin, V. G., G. Milikh, K. Papadopoulos, J. Lyon, Y. S. Dimant, A. S. Sharma, C. Goodrich, and M. Wiltberger (2005b), Effect of anomalous electron heating on the transpolar potential in the LFM global MHD model, *Geophys. Res. Lett.*, *32*, L22,101, doi:10.1029/2005GL023315.
- Merkin, V. G., M. J. Owens, H. E. Spence, W. J. Hughes, and J. M. Quinn (2007), Predicting magnetospheric dynamics with a coupled Sun-to-Earth model: Challenges and first results, *Space Weather*, *5*, S12001, doi:10.1029/2007SW000335.
- Milikh, G. M., and Y. S. Dimant (2003), Model of anomalous electron heating in the E region: 2. Detailed numerical modeling, *J. Geophys. Res.*, *108*, 1351, doi:10.1029/2002JA009527.
- Milikh, G. M., L. P. Goncharenko, Y. S. Dimant, J. P. Thayer, and M. A. McCready (2006), Anomalous electron heating and its effect on the electron density in the auroral electrojet, *Geophys. Res. Lett.*, *33*, 13,809, doi:10.1029/2006GL026530.
- Ober, D. M., N. C. Maynard, and W. J. Burke (2003), Testing the Hill model of transpolar potential saturation, *J. Geophys. Res.*, *108*, 1467, doi:10.1029/2003JA010154.
- Oppenheim, M. M. (1997), Evidence and effects of a wave-driven nonlinear current in the equatorial electrojet, *Ann. Geophys.*, *15*, 899–907.
- Oppenheim, M. M., Y. S. Dimant, Y. Tambouret, and L. P. Dyrud (2011), Kinetic simulations of the Farley-Buneman instability in 3D and the nonlinear wave heating, *J. Geophys. Res.* (to be submitted).
- Pfaff, R. F., M. C. Kelley, E. Kudeki, B. G. Fejer, and K. Baker (1987), Electric field and plasma density measurements in the strongly driven daytime equatorial electrojet, ii - Two-stream waves, *J. Geophys. Res.*, *92*, 13,597–13,612.
- Pfaff, R. F., J. Sahr, J. F. Providakes, W. E. Swartz, D. T. Farley, P. M. Kintner, I. Haggstrom, A. Hedberg, H. Opgenoorth, and G. Holmgren (1992), The E-region Rocket/Radar Instability Study (ERRRIS) - Scientific objectives and campaign overview, *J. Atmos. Terr. Phys.*, *54*, 779–808.
- Pfaff, R. F., J. H. A. Sobral, M. A. Abdu, W. E. Swartz, J. W. Labelle, M. F. Larsen, R. A. Goldberg, and F. J. Schmidlin (1997), The Guar campaign: A series of rocket-radar investigations of the Earth's upper atmosphere at the magnetic equator, *Geophys. Res. Lett.*, *24*, 1663–1667.
- Providakes, J., D. T. Farley, B. G. Fejer, J. Sahr, and W. E. Swartz (1988), Observations of auroral E-region plasma waves and electron heating with EISCAT and a VHF radar interferometer, *J. Atmos. Terr. Phys.*, *50*, 339–347.
- Raeder, J., J. Berchem, and M. Ashour-Abdalla (1998), The Geospace Environment Modeling Grand Challenge: Results from a Global Geospace Circulation Model, *J. Geophys. Res.*, *103*, 14,787–14,798, doi:10.1029/98JA00014.
- Raeder, J. Y., Y. Wang, and F. T. (2001), Geomagnetic storm simulation with a coupled magnetosphere-ionosphere-thermosphere model, in *Space Weather: Progress and Challenges in Research and Applications*, *Geophysical Monograph*, vol. 125, edited by P. Song, H. J. Singer, and G. Siscoe, pp. 377–384, American Geophysical Union, Washington DC.
- Robinson, T. R. (1986), Towards a self-consistent non-linear theory of radar auroral backscatter, *J. Atmos. Terr. Phys.*, *48*, 417–422.
- Robinson, T. R. (1992), The effects of the resonance broadening of Farley-Buneman waves on electron dynamics and heating in the auroral E-region, *J. Atmos. Terr. Phys.*, *54*, 749–757.
- Register, A., and E. Jamin (1975), Two-dimensional nonlinear processes associated with 'type I' irregularities in the equatorial electrojet, *J. Geophys. Res.*, *80*, 1820–1828.
- Rose, G., K. Schlegel, K. Rinnert, H. Kohl, E. Nielsen, G. Dehm, A. Friker, F.-J. Luebken, H. Luehr, and E. Neske (1992), The ROSE project — Scientific objectives and discussion of first results, *J. Atmos. Terr. Phys.*, *54*, 657–667.

- Schlegel, K., and J. P. St.-Maurice (1981), Anomalous heating of the polar E region by unstable plasma waves. I - Observations, *J. Geophys. Res.*, *86*, 1447–1452.
- Schunk, R. W., and A. F. Nagy (2009), *Ionospheres*, Cambridge University Press.
- Siscoe, G. L., G. M. Erickson, B. U. Ö. Sonnerup, N. C. Maynard, J. A. Schoendorf, K. D. Siebert, D. R. Weimer, W. W. White, and G. R. Wilson (2002), Hill model of transpolar potential saturation: Comparisons with MHD simulations, *J. Geophys. Res.*, *107*, 1075, doi:10.1029/2001JA000109.
- St.-Maurice, J. (1987), A unified theory of anomalous resistivity and Joule heating effects in the presence of ionospheric E region irregularities, *J. Geophys. Res.*, *92*, 4533–4542, doi: 10.1029/JA092iA05p04533.
- St.-Maurice, J.-P. (1990), Electron heating by plasma waves in the high latitude E-region and related effects: theory, *Adv. Space Res.*, *10*, 6(239)–6(249).
- St.-Maurice, J.-P., and R. Laher (1985), Are observed broadband plasma wave amplitudes large enough to explain the enhanced electron temperatures of the high-latitude E region?, *J. Geophys. Res.*, *90*, 2843–2850.
- St.-Maurice, J.-P., W. Kofman, and E. Kluzek (1990), Electron heating by plasma waves in the high latitude E-region and related effects: observations, *Adv. Space Phys.*, *10*, 6(225)–6(237).
- Stauning, P., and J. K. Olesen (1989), Observations of the unstable plasma in the disturbed polar E-region, *Physica Scripta*, *40*, 325–332.
- Vanhamäki, H., O. Amm, and A. Viljanen (2007), Role of inductive electric fields and currents in dynamical ionospheric situations, *Ann. Geophys.*, *25*, 437–455, doi:10.5194/angeo-25-437-2007.
- Wang, H., A. J. Ridley, and H. Lühr (2008), Validation of the Space Weather Modeling Framework using observations from CHAMP and DMSP, *Space Weather*, *6*(3), S03,001, doi: 10.1029/2007SW000355.
- Williams, P. J. S., B. Jones, and G. O. L. Jones (1992), The measured relationship between electric field strength and electron temperature in the auroral E-region, *J. Atmos. Terr. Phys.*, *54*, 741–748.
- Winglee, R. M., V. O. Papitashvili, and D. R. Weimer (1997), Comparison of the high-latitude ionospheric electrodynamics inferred from global simulations and semiempirical models for the January 1992 GEM campaign, *J. Geophys. Res.*, *102*, 26,961–26,978, doi:doi:10.1029/97JA02461.

---

Y. S. Dimant, Center for Space Physics, Boston University, 725 Commonwealth Ave., Boston, MA 02215, USA. (dimant@bu.edu)